

## Treball final de grau

**Estudi:** Grau en Enginyeria Química

**Títol:** Integration of gold nanoparticles (AuNPs) in a nanopaper matrix

**Document:** Memòria

**Alumne:** Marina Zamudio Domingo

**Tutor:** Pere Mutjé Pujol; Yves Huttel

**Departament:** Enginyeria Química, Agrària i Tecnologia Alimentària

**Àrea:** Enginyeria Química

**Convocatòria (mes/any):** Juny 2015

## **Acknowledgments**

To everyone who has helped and supported me:

To the LEPAMAP group, for allowing me to pursue this project, especially to my tutor, Pere Mutjé, and to Israel González for counseling me in all the steps needed to complete this work.

To Yves Huttel, Esteban Climent-Pascual and Alicia de Andrés from Instituto de Ciencia de Materials de Madrid for testing our samples with the SPR technique.

And finally, to all the people, especially to my family and friends, who have helped me during these last months to achieve this Chemical Engineering degree here at Universitat de Girona. I love you very much! The future is ours!

---

## Table of contents

1. Introduction and objectives .....	5
1.1 Background .....	5
1.2 Objective .....	6
1.3 Scope .....	6
2. Theoretical foundings.....	8
2.1 Cellulose nanofibers .....	8
2.1.1 Hardwood and softwood .....	11
2.1.2 Production methods .....	12
2.1.3 CNF properties and application.....	16
2.1.4 Nanopaper .....	21
2.2 Gold nanoparticles (AuNPs) .....	24
2.2.1 Synthesis of AuNPs .....	24
2.2.2 Properties and applications of the AuNPs.....	26
2.2.3 Functionalized nanopapers with AuNPs .....	29
2.3 Surface Plasmon (SPs) and Surface Plasmon Resonance (SPR) .....	31
3. State of the art .....	33
4. Materials and methods.....	38
4.1 Materials.....	38
4.2 Methods.....	41
4.2.1 Pulp preparation.....	41
4.2.2 Consistency .....	42

---

4.2.3	Obtention of CNF .....	43
4.2.4	CNF characterization .....	47
4.2.5	Nanopaper formation and characterization .....	55
5.	Results and discussion .....	61
5.1	CNF characterization .....	61
5.1.1	Consistency .....	61
5.1.2	Yield of fibrillation .....	61
5.1.3	Carboxylic group content .....	63
5.1.4	Cationic demand .....	64
5.1.5	Degree of polymerization .....	64
5.2	Nanopaper characterization .....	66
5.2.1	Morphology .....	66
5.2.2	Transmittance .....	67
5.2.3	Mechanical properties .....	68
5.2.4	Surface Plasmon resonance .....	70
5.3	AuNP/nanopaper composite characterization .....	71
5.3.1	Morphology .....	71
5.3.2	Transmittance .....	72
5.3.3	Mechanical properties .....	74
5.3.4	Surface plasmon resonance .....	76
6.	Conclusions .....	79
7.	Costs estimation .....	82

8. Evolution of the project: Gantt diagram ..... 86

9. Bibliography ..... 87

---

# 1. INTRODUCTION AND OBJECTIVES

## 1.1 Background

During the last 15 years, there has been a tremendous growth in the field of biosensor research due to their potential use in fields such as medical diagnosis, environmental control and food safety. The development of low-cost, accurate and sensitive diagnostic tests is crucial to these applications, in particular in those for the industry, or for upscaling these processes.

Significant opportunities exist for the development of new composite natural fiber materials comprising a conventional nanofiber substrate, which has been functionalized with nanomaterials, to impart particular chemical, optical, catalytic, sensing, and antimicrobial properties. A product that within the last 10 years has attracted this field of research have been the cellulose nanofibers (CNF), which are defined for its 5-100 nm diameter and a few micrometers of longitude.

The CNF come from the mechanical disintegration of the conventional microfibers which, to help their disintegration, are treated with chemical or enzymatic pre-treatments which also helps to lower the process energetic consumption. Apart from that, its raw material is renewable, it can be wood fibers, fibers from recycled paper or residual fibers among others. With a good dispersion of these nanofibers, nanopapers can be formed. Nanopapers are transparent membranes made entirely of CNF that are usually fabricated by using vacuum-assisted filtration technique or evaporation at room temperature for production of transparent paper sheets.

Another nanomaterial studied in the last decades are gold nanoparticles (AuNPs). Colloidal gold nanoparticles have been utilized for centuries by artists due to the vibrant colors produced by their interaction with visible light. More recently, these unique optical-electronic properties have been researched and utilized in high technology applications such as organic photovoltaics, sensory probes, therapeutic

agents, drug delivery in biological and medical applications, electronic conductors and catalysis.

AuNPs exhibit excellent physic, chemical and biological properties that are intrinsic of its nanometric size. The most unexpected properties of AuNPs are the photothermal properties, activated in presence of laser light. Using these characteristics, AuNPs have, for example, been used for the scientific community on the investigation and application of AuNPs in the detection, diagnosis and treatment of cancer.

The good integration of these two nanomaterials, could derive into a new composite which could be used on the applications explained above.

## **1.2 Objective**

The main objective of the present TFG is to create a new functionalized nanopaper with different percentages of AuNPs and to assess their properties, such as physical, optical and mechanical.

CNF with different levels of oxidation will be obtained from pine and eucalyptus bleached fibers. These obtained nanofibers will be characterized and afterwards they will be used to form nanopapers. Six different types of nanopapers will be fabricated as to determine how the addition of different quantities AuNPs affects the properties of the composite.

## **1.3 Scope**

The scope of this work consists on introducing the cellulose nanofibers, nanopaper, AuNPs and functionalized nanopapers concepts, determine the state of the art of the nanocellulose/AuNPs composite and the characterization of the obtained CNF and nanopapers.

To characterize the CNF the yield of fibrillation, the carboxylic group amount, the cationic demand and the polymerization degree will be studied.

To characterize the different nanopapers the thickness, the density, the transmittance the FE-SEM microphotographs, the mechanical properties and the surface plasmon resonance will be studied.

## 2. THEORETICAL FOUNDINGS

### 2.1 Cellulose nanofibers

In recent years, the interest of new bio-based renewable materials has increased (Missoum *et al.* 2013). Environmental concerns and a reduction of the dependency on oil are two important factors that have influenced the need of developing renewable, green, biodegradable materials (Alemdar & Sain, 2007, Spence *et al.* 2011, Zhang *et al.* 2012, Abdul Khalil *et al.* 2014). In particular, cellulose has gathered special attention in the last decade.

As a biopolymer, cellulose is formed by the repetition of glucose units linked together by glycosidic bonds ( $\beta$  1 $\rightarrow$ 4) forming a linear macromolecule. Figure 2.1 shows the general structure of the cellulose chain. The union of two of these glucose units is called cellobiose, and is considered as the monomer of cellulose. The polymeric nature of cellulose was revealed by German chemist Hermann Staudinger in 1920 through acetylation and desacetylation reactions on cellulose. With his experiments, he demonstrated that the glucose units did not merely formed aggregates, but long, molecular chains linked together by acetal covalent bonds.

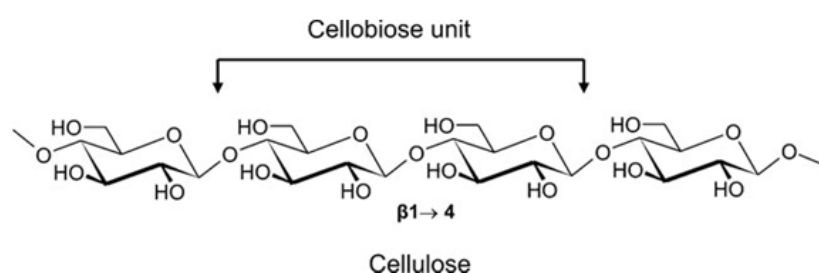


Figure 2.1. Cellulose representation (<http://www.namrata.co/wp-content/uploads/2012/04/D1.bmp>)

The degree of polymerization of cellulose ( $DP$ ) varies depending on the source and treatment of the original cellulose fibre. Usual  $DP$  values in wood pulp are reported to be between 300 and 1700. In nature, cellulose has a  $DP$  of approximately 10000 glucopyranose units in wood cellulose and of 15000 units in plant cellulose, whereas bacterial cellulose shows  $DP$  values of 2000-6000 (Yoshinaga *et al.* 1997, Iguchi *et al.*

2000). A polymer chain of 20-30 D-Glucose units already presents all the properties of cellulose. The original cellulose chain can be depolymerized by acid treatment and enzymatic hydrolysis.

The presence of polar –OH groups along the cellulose chain provides many of the very well-known properties of this biopolymer, such as hydrophilicity, chirability, degradability and chemical reactivity. Besides, –OH groups are also responsible for the formation of hydrogen bonds between chains, allowing the cellulose chain to adopt highly crystalline structures that ultimately define the mechanical properties of cellulose (O’Sullivan, 1997).

In biological structures, cellulose is produced as highly crystalline nanofibrils consisting of fully extended and uniaxially aligned cellulose molecules (Saito et al. 2012) that alternate crystalline regions with amorphous ones. Such nanofibrils, also called elementary fibrils, have diameters ranging between 3 and 5 nm and consist of 30-40 cellulose chains (Isogai et al. 2011).

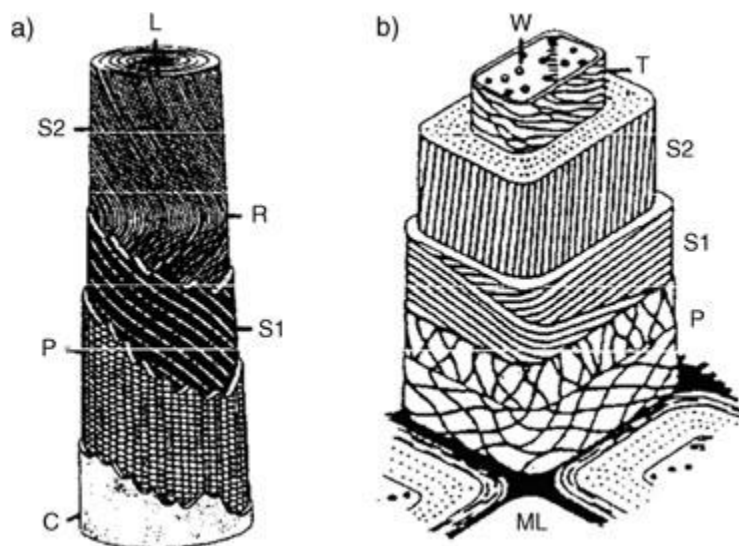


**Figure 2.2. Structure of plant cell walls from a) cotton linters and b) wood fibre: C, cuticula layer; L, lumen; ML, middle lamella; P, primary cell wall layer; R, reversing point; S1, secondary cell wall layer 1; S2, secondary cell wall layer 2; T, tertiary cell wall; W, wart layer (Klemm et al. 2005).**

The width of microfibrils depends on the biologically intrinsic arrangements of the terminal complexes, which are cellular membrane structures that synthesize cellulose (Iwamoto *et al.* 2009). Microfibrils are organized in macrofibrils, whose diameter varies between 10 and 30 nm; aggregates of macrofibrils present diameters of 100 nm or more. Microfibrils and their aggregates can reach lengths of several hundreds of nm (Klemm *et al.* 2005).

The term cellulose nanofibres (CNF) or microfibrillated cellulose (MFC) is applied to aqueous suspensions where cellulose fibers (usually from bleached wood pulps) have been disintegrated until the microfibrils are released from the plant cell wall.

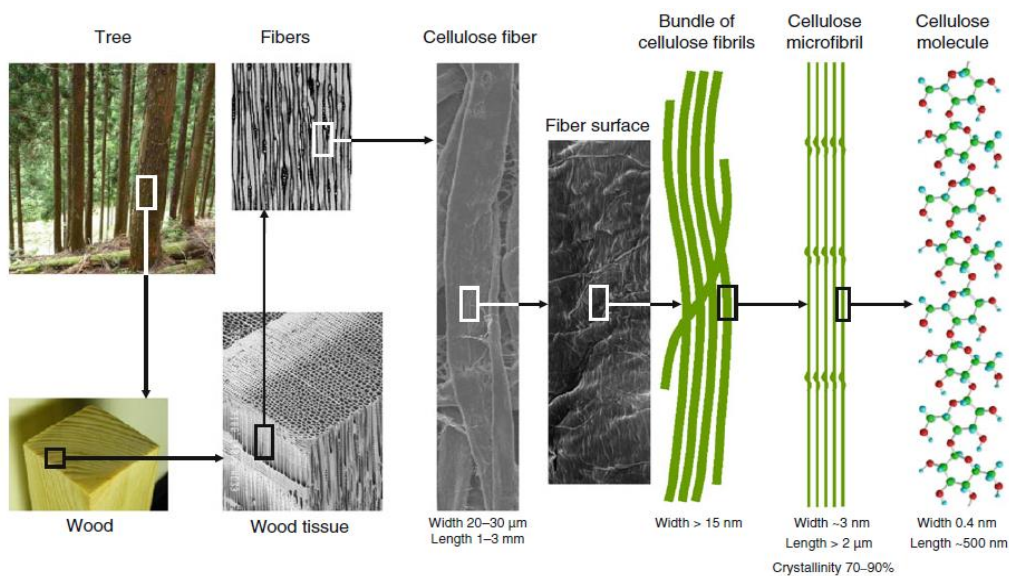


**Figure 2.3. From the tree to the cellulose molecule scheme (Isogai *et al.* 2010).**

These microfibrils suspensions already form gel-like substances at very low (0.5-2 wt %) concentrations. The term microfibrillated cellulose was initially applied by Turbak *et al.* (1983) in the first reports about this new material and denoted that MFC was a cellulose suspension where microfibrils had been isolated from the larger fibres. However, the acronym MFC can lead to think that the size range of these cellulose fibres is in the micrometric scale. The kind of fibres reported by Turbak *et al.* was described as having diameters below 0.1  $\mu\text{m}$ ; this measure fits well into the nanoscale, which refers to materials with sizes between 0.001 and 0.1  $\mu\text{m}$  (Chinga-Carrasco

2011). Therefore, it is clear that microfibrils can be also called nanofibrils. The main difference between both terms is that microfibrils is a well-defined biological structure found in plant cell walls, whereas nanofibril is a technological term created in order to describe secondary engineered fibers with diameters less than 0.1  $\mu\text{m}$  (Chinga-Carrasco 2011). MFC and NFC are still widely used in specialized literature, along with other terms such as microfibrillar cellulose, nanocelluloses, cellulose nanofibres and nanofibrillar cellulose (Taipale *et al.* 2010). The term cellulose nanofibres and consequently its acronym CNF are preferred in the present work since both terms emphasize the nanometric nature of this material.

Bacterial cellulose and cellulose whiskers found in tunicates are also naturally presented as nanofibril-networks (Eichorn *et al.* 2010). Diameters in CNF vary from that of a single microfibril (3-5 nm) to thicker microfibril aggregates of up to 100 nm (Saito *et al.* 2011, Klemm *et al.* 2011, Abdul Khalil *et al.* 2014). Lengths can be of several hundreds of nm to 1  $\mu\text{m}$ .

### 2.1.1 Hardwood and softwood

Traditionally, the main source of cellulose fibers for the papermaking industry is kraft wood pulp, either from the so called hardwoods (mainly eucalyptus) and softwoods (pine). Though the terms softwood and hardwood may indicate that the former are “stronger”, they actually refer to the density of wood, being hardwood, in general denser than softwood. However, this definition does not apply to all hardwood and softwood, since many softwood species are in fact denser than hardwood ones. Softwood is obtained from gymnosperm trees that present needle-like leaves that do not fall during autumn-winter. Softwood presents medullary rays and tracheid that transport water and produce sap.

Fibers from softwood and hardwood also present significant differences. In general, softwood fibers are larger and thicker (3.5 mm length and 40 microns width) than hardwood ones (1 mm length and 20 microns width) (Shackfort 2003). The fiber wall

thickness is generally highly variable in softwood pulps due primarily to the large difference in fiber properties from early wood and late wood, with the latewood being much narrower fibers with very thick walls (Shackford 2003). The cellulose fraction of wood in hardwood pulps is slightly higher than in softwoods, but the total cellulose and hemicellulose fraction is similar in both types of pulpwood.

### 2.1.2 Production methods

The first reports on the fabrication of CNF suspensions were made in the late 70's and early 80's at ITT Rayonier, USA, by Turback and Herrick (Qua *et al.* 2011, Spence *et al.* 2011). Such suspensions were prepared by passing a wood-fiber suspension through high-pressure homogenizers. This process produced extensive delamination of the cell wall, ultimately liberating the microfibrils. The microfibrils present high aspect ratio and their water suspensions show thixotropic and pseudoplastic behavior (Klemm *et al.* 2011).

When this new material was first developed, the main drawback found for its large-scale production was the high-energy consumption needed during the homogenization process. This was so because wood pulp suspensions required numerous passes through the homogenizer to liberate the microfibrils. Clogging of the homogenizer was also a recurring problem during the fabrication of CNF (Klemm *et al.* 2011, Spence *et al.* 2011).

During the following years, attempts were made to reduce the energy consumption during the delamination step. Other equipments such as microfluidizers, grinders and mills have also been used for effectively releasing the microfibrils. However, it became clear that previous treatment of the cellulose fiber was necessary in order to diminish the high-energy consumption by reducing the number of passes that wood pulps required.

Mechanical, chemical and enzymatic pre-treatments are nowadays used to reduce the fiber size and/or to pre-defibrillate the fibers, reducing the number of passes and clogging (Spence *et al.* 2011). Mechanical pre-treatments include passing the wood

pulp previously through disk refiners, PFI mills, manual cutting and Valley beaters. Regarding chemical pre-treatments, TEMPO-mediated oxidation and carboxymethylation of cellulose are the two most used methodologies. Chemical pre-treatments induce swelling of fibers, facilitating thus the mechanical defibrillation (Saito *et al.* 2007). Enzymatic treatment has also been reported as an effective pre-treatment before mechanical delamination (Henriksson *et al.* 2007).

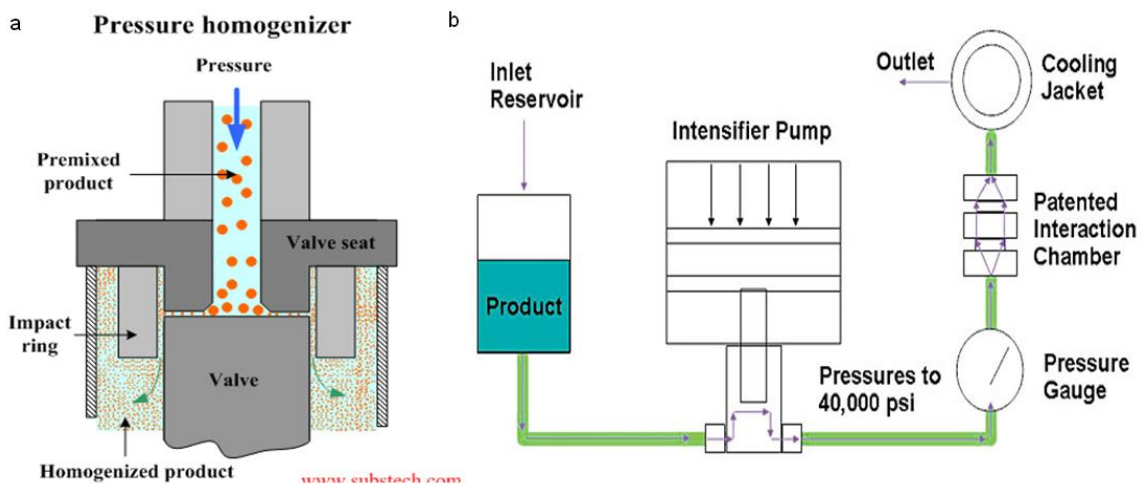


Figure 2.4. Homogenization procedure (<http://www.chem.info>).

The most used mechanical treatments reported in the literature are high-pressure homogenization and microfluidization (Figure 2.4). The first method consists in passing the cellulose slurry at high pressure into a vessel through a very small nozzle. High velocity and pressure as well as impact and shear forces on fluid generate shear rates in the stream and decrease the size of fibers to nanoscale (Abdul Khalil 2014). Some of the advantages of this method include high efficiency and simplicity. Pressures of up to 30-50 MPa are achieved during homogenization, and temperature of the fluid can be as high as 75°C.

Grinding is another mechanical system formed by a static and a rotating grinding stone and the cellulose slurry is forced through these two stones. Once again, friction and shear forces are involved in the delamination of the cellulose fiber. As in the aforementioned methods, several passes through the grinder are necessary to obtain

CNF. Finally, cryocrushing and high intensity ultrasonication are two more marginal methods reported in literature as effective to fabricate CNF. In cryocrushing, the cellulose slurry is frozen with liquid nitrogen and subsequently crushed by mortar and pestle. High intensity sonication requires the use application of ultrasounds to the cellulose slurry where the ultrasound-induced cavitation leads to a powerful mechanical oscillating power and high intensity waves, which consist of formation, expansion and implosion of microscopic gas bubbles when molecules absorb ultrasonic energy (Abdul Khalil 2014).

### **2.1.2.1 Pre-treatment**

As mentioned before, CNF was first obtained after passing a wood pulp suspension through a high-pressure homogenizer until obtaining a gel-like substance. However, this process required passing the pulps suspension many times through the homogenizer, which represented important energy consumption. Nowadays is generally accepted that, in order to reduce the energy needed to mechanically release the microfibrils, a pre-treatment should be previously applied on the fibers. Values around 20,000-30,000 kWh/tonne are not uncommon (Sirò & Plackett 2010). Higher values have also been reported. By applying chemical or enzymatic it is possible to reduce the energy consumption to 1,000 kWh/tonne (Ankerfors & Lindström 2007). The most important types investigated up to now are alkaline/acid pre-treatment, enzymatic hydrolysis and TEMPO-mediated oxidation.

### **2.1.2.2 Alkaline, acid and enzymatic pre-treatments**

In the alkaline pre-treatment, fibers are heated at 80°C for 2 hours in a 2% (w/w) NaOH solution; the main objective of this treatment is to eliminate pectin substances, hemicelluloses and phenolic molecules like pectin and polyphenols (Alendar & Sain 2008, Dufresne *et al.* 1997, Wang & Sain 2007). The resulting treated fibers were then passed through a high-pressure homogenizer at 500-1000 bars of pressure; up to 20 passes were required to crush the cell wall and fully release the microfibrils (Wang & Sain 2007). A key factor in this method is to control the NaOH addition, its concentration and temperature; too concentrated solutions or higher reaction times tend to partially degrade cellulose via  $\beta$ -elimination (Dufresne *et al.* 1997). The 2%

NaOH solution is reported to be low enough to avoid cellulose degradation. Alkaline pre-treatment can be followed by bleaching with  $\text{NaClO}_2$  and beating with a PFI-mill at 12,000 revolutions (Wang & Sain 2007) before the homogenization step.

Acid hydrolysis has been extensively applied for isolation of cellulose nanocrystals (whiskers); nevertheless, very few works have isolated cellulose nanofibres using this technique. Of those works, Zimmermman et al. reported obtaining CNF from sulphite wood pulp treated with a 10% sulphuric acid solution at 60°C under constant stirring during 16 hours. The suspension was then rinsed, neutralized and homogenized at 1000 bars for 16 minutes. The resulting nanofibres were below 50 nm diameter, with polymerization degrees of 300. The reinforcing effect of CNF in nanocomposites was also studied, resulting in improvement of mechanical properties of several polymeric matrices.

Another approach to facilitate the mechanical treatment of cellulose pulps is the enzymatic treatment. The use of enzymes previous to mechanical beating is a well-known technology in the papermaking industry. Specifically, the endoglucanases catalyse the hydrolysis of the glycosidic bonds ( $\beta$  [1→ 4]) connecting each glucopyranose molecule constituting the cellulose chain. They are used on cellulose pulps in order to reduce the amount of beating needed to increase the mechanical properties of the slurry. The enzymatic pre-treatment requires the use of cellulases that hydrolyze the amorphous regions of the cellulose chains, causing a slight internal and external fibrillation of the fibers and increased water absorbency.

### **2.1.2.3 TEMPO-mediated oxidation**

From all the pre-treatments mentioned above, TEMPO-mediated oxidation is one of the most used methods nowadays. It has been reported by many authors as a very effective, easy to control method to prepare cellulose fibers for mechanical treatment (Saito *et al.* 2007, Besbes *et al.* 2011a, Isogai *et al.* 2011, Syverud *et al.* 2011, Zhang *et al.* 2012, Alila *et al.* 2013).

Basically, the reaction oxidizes the C6 of the D-Glucose unit by substituting the –OH group of that carbon for a COOH group. The reaction uses either NaClO or NaClO<sub>2</sub> as oxidizers; the reagent TEMPO (2,2,6,6-tetramethylpiperidine-1-oxyl radical) as a catalyst. TEMPO and its analogues are water-soluble, commercially available and stable nitroxyl radicals, most of which have a negative result to the Ames test (Isogai *et al.* 2011). The oxidation of polysaccharides to yield polyuronic acids has been studied for more than a half-century (Da Silva *et al.* 2003). Nooy *et al.* in particular, first applied TEMPO-mediated oxidation to water-soluble polysaccharides such as starch, amylopectin and pullulan for regioselective conversion of C6 primary alcohol to carboxylate groups (Isogai *et al.* 2011).

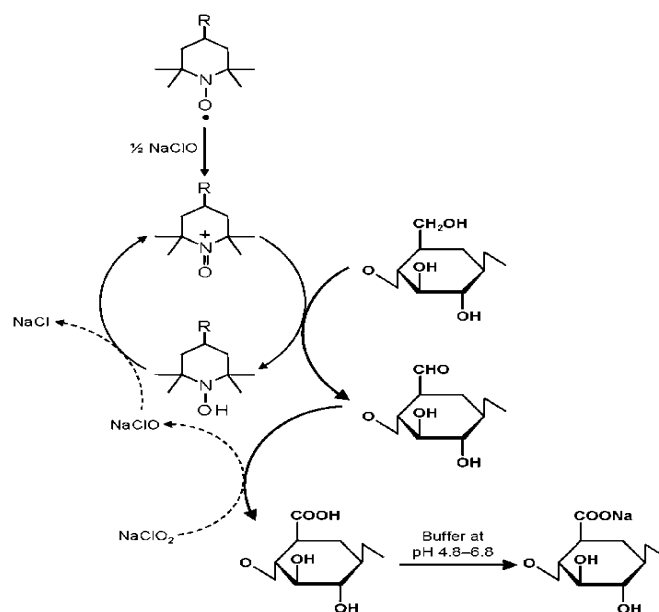


Figure 2.5. TEMPO oxidation chemical process (Isogai *et al.* 2011).

### 2.1.3 CNF properties and application

All the properties of cellulose are expected to be present in CNF. The intrinsic properties of nanofibrillated cellulose have attracted special attention during the last years. Their nanometric size and high aspect ratio, along with their low density (1.5 g/cm<sup>3</sup>), high crystal moduli (130-150 GPa), low coefficient of thermal expansion (6 ppm K<sup>-1</sup>) and large surface areas (approx. 1000 m<sup>2</sup> g<sup>-1</sup>) have found applications on different

fields, such as paper additives, composite materials, oxygen barriers, shock absorbers and high-capacity supports for catalyst, conducting and magnetic materials (Saito *et al.* 2012, Abdul Khalil *et al.* 2014). The size of CNF is usually determined via electronic microscopy, either field emission scanning electron microscopy (FE-SEM), transmission electron microscopy (TEM) or atomic force microscopy (AFM). The widths of CNF can vary from that of a single microfibril (3-5 nm) to 10 or more nm that corresponds to microfibrils aggregates. The width distribution can be determined by computerized image analysis; however, length distributions are hard to calculate due to the entanglement of CNF and the difficulty to differentiate both ends of a single microfibril. CNF prepared from TEMPO-oxidized celluloses is reported to have very uniform width distributions (Isogai *et al.* 2011).

The *DP* of CNF depends upon the cellulose source and the kind of treatment used for the manufacturing of the CNF. An important decrease in the *DP* of CNF in comparison with the original cellulose source is always expected. For cellulosic materials, the *DP* is usually calculated from the intrinsic viscosity ( $\eta$ ) from cellulose solutions in cupri-ethylene diamine. The CNF fabricated from TEMPO-oxidized celluloses at alkaline conditions usually presents the greatest depolymerisation (Isogai *et al.* 2011, Syverud *et al.* 2011). CNF from enzyme-treated pulps or TEMPO-oxidized pulps under neutral conditions shows moderate to low depolymerisation. The *DP* of CNF is an important parameter because it determines the intrinsic strength of the fibre and therefore the ultimate tensile strength of nanopapers made thereof (Henriksson *et al.* 2008).

The *cationic demand* equals the amount of highly charged cationic polymer required to neutralize its surface. The cationic demand is measured by polyelectrolyte titration and was initially developed to measure the charge density of polyelectrolytes and later applied to charge titrations on fibre materials (Klemm *et al.* 2011). This methodology is based on the fact that polyelectrolytes can form complexes with oppositely charged polyelectrolytes (direct titration) or surfaces (indirect titration). Stoichiometry is attained only if the ionic strengths are low enough to allow the charge fields to overlap. Another condition to be accomplished is that the molecular weight of the polyelectrolyte must be sufficiently high that the molecule cannot penetrate the cell wall surface of cellulose fibres. The cationic demand allows determining the extent of cell-wall delamination and

it is typically applied on beaten pulps to know the beaten degree. In the case of CNF, the cationic demand increases with the number of passes through a homogenizer. Moreover, in the case of TEMPO-oxidized fibres, the cationic demand increases with the content of carboxylic groups. As expected, due to their larger specific surface area, CNF presents higher cationic demands than beaten pulps.

The colloidal stability of CNF has also been intensely studied. Since CNF is usually produced as gel-like aqueous suspensions due to its strong affinity to water, to control aggregation and gelation of aqueous CNF suspensions has become a matter of study. It has been demonstrated that CNF tend to form aggregates at low pH or elevated concentration. In low pH environments, the bulk concentration of protons increases and this increase is accentuated around the CNF surface because of electrostatic attraction. This leads to protonation of carboxylic groups and consequently reduction in both the surface charge and the electrostatic repulsion between nanofibers, which finally induce nanofiber aggregation (Fall *et al.* 2011). The addition of salt into the medium generates a high concentration of counterions near the nanofiber surface due to electrostatic attraction. Specific interactions between counterions and carboxylic groups are significantly weaker than proton-carboxylic interactions. However, they are important for the charged CNF due to the improved ion concentration close to the nanofiber surface. The surface charge then decreases, causing aggregation at high concentration of CNF. This effect is much stronger than the electrostatic screening of the diffusive layer, which was previously believed to be dominant (Fall *et al.* 2011).

Polymer adsorption of CNF aqueous suspensions is another important property. Nanofibers tend to form polyelectrolyte multilayers (PEM's) which are structures formed by particles with oppositely-charged surfaces (Wågberg *et al.* 2008). It is possible to prepare PEM's with CNF by adding different cationic polyelectrolytes such as poly-DADMAC (polydiallyldimethylammonium chloride), PAH (poly-allylamine hydrochloride), PEI (polyethyleneimine), xyloglucan and cationic starch (Ahola *et al.* 2008a, Wågberg *et al.* 2008). The type of polymer used for the formation of PEM's has a strong effect on the properties of the film layer formed on nanofibers' surface and water content on the interfacial level and nanofiber aggregation on a more microscopic level (Ahola *et al.* 2008a). The combination of PEI and CNF results in the formation of

regular layers of nanofibers and PEI with layer thickness of 20 and 3 nm, respectively, after deposition of about 10 layers (Wågberg *et al.* 2008). Salt concentration influences the thickness of PEM's formed by adsorption of poly-DADMAC and PAH.

The mechanical properties of CNF have been intensely studied during the last years. This is a very important property because it determines the strengthening ability of CNF when used as reinforcement in nanocomposites. Regarding Young's modulus, the first attempts to determine this parameter in cellulose crystals dates back to 1936 when Meyer and Lotmar used a model and bond stiffness constants derived from spectroscopic measurements (Eichhorn *et al.* 2010). The authors calculated a value of roughly 120 GPa, a value very close to the ones calculated years later. The problem with this value is that it was calculated using an erroneous structure for cellulose; this was later corrected by Lyons, who calculated a new value of 180 GPa. However, he used an incorrect term in his mathematical expression for bond angle bending. This problem was fixed by Treloar, reporting a modulus of 56 GPa. This value, however, is nowadays considered as too low (Eichhorn *et al.* 2011); it is likely that Treolar did not take into consideration the intramolecular hydrogen bonding in his cellulose structure. Sakurada *et al.* (1962) determined the modulus of crystal cellulose by X-ray diffraction, reporting a value of 138 GPa.

Later X-ray studies and theoretical considerations from other authors have determined that Young's modulus of crystalline cellulose ranges from 100 to 160 GPa depending on the source and the method used for the calculation. A higher Young's modulus was determined by Diddens *et al.* (2008), who reported a value of 220 GPa calculated using X-ray scattering. This value would be correct if we assume that stress is uniformly distributed along the surface of the cellulose crystal, which, in fact, does not occur (Eichhorn *et al.* 2010). Regardless of such disparities, it is clear that CNF present a high modulus comparable and even superior to those of other engineering materials such as aluminium and glass (69 GPa) and steel (200 GPa). Moreover, if we consider cellulose's low density (1.5 g/cm<sup>3</sup>) and compare it to that of aluminium (2.7), glass (2.5) and steel (7.8), we can see that cellulose has a large specific modulus (modulus/density) than the other materials.

In contrast to Young's modulus, the tensile strength of a single nanofiber has not been extensively studied (Saito *et al.* 2012). A possible explanation to this could be that, until recently, it was very difficult to isolate cellulose microfibrils. The most recent attempts to determine the tensile strength of a single CNF were those of Saito *et al.* 2012 who calculated the tensile strength of single microfibrils prepared from TEMPO-mediated oxidized wood fibres and native cellulose CNF isolated from marine tunicates. The method to calculate the tensile strength was based on a model for the sonication-induced fragmentations of filamentous nanostructures. The resulting strength parameters were then analysed based on fracture statistics. The results indicated that the mean tensile strength of wood cellulose CNF ranged from 1.6 to 3 GPa, depending on the method used to measure the microfibril width. In contrast, the highly crystalline, thick tunicate CNF showed mean strength of 3 to 6 GPa. According to the author, tensile strength values of 1 GPa are reasonable considering that CNF films (which are firmly hydrogen-bonded to each other) have a tensile strength of 0.1 to 0.4 GPa and the maximum tensile strength of a given material corresponds to roughly one tenth of the elastic modulus. The difference in strength between CNF from wood pulp and tunicates might be a consequence of the type of pre-treatment that wood pulps undergo to obtain CNF. After the TEMPO-mediated oxidation, the surface of cellulose fibres is chemically modified which might lower the intrinsic strength of nanofibers. Moreover, the use of sonication in that study introduces mechanical defects in the cellulose nanofibers including kinks and delamination of the molecular sheets. Such defects may initiate tensile fracturing, which is the dominant mechanism of sonication-induced fragmentation (Saito *et al.* 2012).

There are different sources and techniques to obtain CNF that can be combined. This fact, facilitates a broad spectrum of CNF with different sizes and properties that can be produced to serve in different fields and applications.

Normally the CNF are applied on:

- Foams and aerogels to provide a bigger specific area to enhance its properties. Depending on its density, they would be applied on sound insulation, fire retardant, gas barrier (Svagan, Samir *et al.* 2008).

- Materials where the oxygen selective barrier property is important (Fukuzumi, Saito *et al.* 2009).
- Hybrid magnetic nanoparticles models (Olsson, Samir *et al.* 2010).
- Coating for high quality printing. The hydrophilic properties of CNF enable the ink to expand in a controlled way (Luu, Bousfield *et al.*). Also, CNF have been studied for its application in materials which are used in electronic printing with silver nanoparticles as ink (Torvinen, Sievänen *et al.* 2012).
- Optical materials, due to the transparency of CNF. This property is caused because its length is approximately half of the wavelength of radiation in the visible spectrum. The CNF can be impregnated into Epoxi and acrylic resins to produce optical materials optics (Yano, Sugiyama *et al.* 2005).

#### 2.1.4 Nanopaper

The word nanopaper is a term that has been recently created to describe membranes made entirely or almost entirely of CNF. Nanopapers are formed when the water of a CNF suspension is removed so that a cellulose nanofibril network is formed, firmly held together by hydrogen bonds. Nanopapers are usually fabricated by either using vacuum-assisted filtration technique for production of paper sheets (Henriksson *et al.* 2008, Chinga-Carrasco & Syverud 2009, Sehaqui *et al.* 2010, Chun *et al.* 2011, Ferrer *et al.* 2012, Kulachenko *et al.* 2012, Fang *et al.* 2013, Varanasi & Batchelor 2013) or by casting and evaporation at room temperature or inside an oven (Dufresne *et al.* 1996, Syverud *et al.* 2011, Kumar *et al.* 2014).

Nanopapers present different properties in comparison to ordinary papers due to the nanometric nature cellulose nanofibers. Nanopapers present smoother surfaces, high densities close to that of cellulose (1.5 g/cm<sup>3</sup>), high transparency and compactness. Mechanical properties are also significantly higher than ordinary papers. Cellulose nanofibres in nanopapers present a random-in-the-plane, layered structure where nanofibers' ends are difficult to discern. Though the term nanopaper appeared in 2008 (Henriksson *et al.* 2008), the fabrication of CNF membranes had already been explored. Dufresne *et al.* (1996) prepared sheets from sugar beet cellulose microfibrils

and investigated their tensile properties. In that work, microfibrils were prepared using an alkaline treatment followed by shear disintegration with a homogenizer and by cryocrushing. CNF Films were later prepared by casting and drying at 37°C. Among other results, Young's modulus increased with the duration of the mechanical treatment of the pulp due to a higher individualization of the microfibrils and then to the formation of a network of cellulose microfibrils within the material; however, the results presented were somehow low in comparison with modern nanopapers.

Chinga-Carrasco & Syverud (2009) studied in detail the different scales of organization that nanofibres adopt in a nanopaper. Several devices such as desktop scanner, scanning electron microscopy and backscatter electron microscopy, among others, were used for the visual characterization of the samples. The results indicated the random orientations of nanofibres in the nanopaper and the layered arrangement that they adopt. Besides, it was also demonstrated the difficulties of determining the real thickness of nanopapers due to irregularities on the nanopaper's surface. This fact can induce to miscalculation of the cross section of a nanopaper and thus lead to misinterpretation of its mechanical properties.

One of the main early drawbacks found in the fabrication of CNF was that long drainage times were required to remove most of the water from the CNF suspension, ranging from a few hours to a whole day, whereas evaporation at room temperature can take several days. However, some authors have reported faster methodologies for the fabrication of nanopapers. Sehaqui *et al.* (2010) reported the fabrication of nanopapers using a semi-automatic Rapid-Köthen-like sheet former provided also with a 0.65 µm pore diameter nitrocellulose membrane. The authors reported that it took about 45 minutes to produce nanopapers of 60 µm width and 20 cm diameter. The mechanical and physical properties of nanopapers fabricated using this methodology were compared to other samples prepared by following different systems, namely casting, filtration+oven drying and filtration+hot pressing. Nanopapers fabricated using the described methodology presented high tensile strength (up to 232 MPa) and Young's modulus (13.4 GPa), whereas transparency was also high. The same method was used to prepare nanocomposites of CNF and nanoclays.

The transparency and high resistance of nanopapers have raised interest in the field of flexible electronic devices. Fang *et al.* (2013) developed the first writable nanopaper with high smoothness and optical transmittance by fabricating a bilayer hybrid paper using unbeaten wood fibers and CNF with a papermaking technique. From this material, the authors fabricated a transparent paper touchscreen with excellent anti-glare effect in bright environments. Electric conductivity in nanopapers was achieved by adding a fine layer of carbon nanotubes.

Kumar *et al.* (2014) compared the properties of films made out of nanofibrillated cellulose and microfibrillated cellulose. The first were prepared using TEMPO-mediated oxidation as pre-treatment followed by high pressure homogenization, whereas MFC was produced using a mechanical treatment only. The TEMPO-mediated oxidation of softwood and hardwood produced very similar CNF; these films showed superior mechanical and optical properties than MFC films, though the last ones demonstrated better barrier properties against oxygen and water vapor. Both kinds of films were very effective barriers against oxygen, water vapor and mineral oils used in ordinary printing inks and dichlorobenzene, a common solvent used in functional printing inks.

## 2.2 Gold nanoparticles (AuNPs)

The nanoparticles of noble metals and, specifically, gold nanoparticles (AuNPs), exhibit excellent physic, chemical and biological properties that are intrinsic of its nanometric size. The most unexpected properties of AuNPs are the photothermal properties, that when activated in presence of laser light, radiate heat as if they were <<nano-heaters>>. AuNPs can be produced with different sizes and shapes and are easily functionalized with a lot of ligands (antibodies, polymers, diagnostic catheters, drugs...). Therefore, AuNPs are of great interest in the biomedicine field among others.

The AuNPs have an extraordinary potential as phototherapeutic agents on cancer treatment as well as in the elaboration of nanostructures for the transportation and selective vectorization of drugs and therapeutic macromolecules and in genic therapy. They could also play an important role on the elaboration of <<intelligent transportation systems>> that permit to control, in space and time, the release of the associated therapeutic agent thanks to and internal biological stimulus.

On the last years, the scientific community has leaded several efforts to the investigation and application of AuNPs in the detection, diagnosis and treatment of cancer.

### 2.2.1 Synthesis of AuNPs

A wide array of solution based approaches has been developed in the past few decades to control as the size, shape, and surface functionality. Turkevich et al. developed a synthetic method for creating AuNPs in 1951 by treating hydrogen tetrachloroaurate ( $\text{HAuCl}_4$ ) with citric acid in boiling water, where the citrate acts as both reducing and stabilizing agent (Figure 2.6). Frens further refined this method by changing the gold-to-citrate ratio to control particle size. This protocol has been widely employed to prepare dilute solutions of moderately stable spherical AuNPs with diameters of 10 to 20 nm, though larger AuNPs (e.g., 100 nm) can also be prepared. These citrate-stabilized AuNPs can undergo irreversible aggregation during functionalization process with thiolate ligands. Several strategies have been developed

to conquer this problem including using a surfactant, Tween 20, prior to the modification to prevent aggregation (Figure 2.6), or using thioctic acid as an intermediate via a two step functionalization. However, the requirement for high dilution makes large scale production challenging.

Brust and Schriffin achieved a breakthrough in AuNP synthesis in 1994 by creating organic soluble alkane thiol-stabilized AuNPs through a biphasic reduction protocol using tetraoctylammonium bromide (TOAB) as the phase transfer reagent and sodium borohydride ( $\text{NaBH}_4$ ) as the reducing agent (Figure 2.6). This methodology produces low dispersity AuNPs from 1.5 to 5 nm by varying the reaction conditions such as gold-to-thiol ratio, reduction rate, and reaction temperature.

These alkanethiol-protected AuNPs possess higher stability when compared to most other AuNPs due to the synergic effect of the strong thiol-gold interactions and van der Waals attractions between the neighboring ligands. These nanoparticles can be thoroughly dried and redispersed in solution without any aggregation making them excellent precursors for further functionalization.

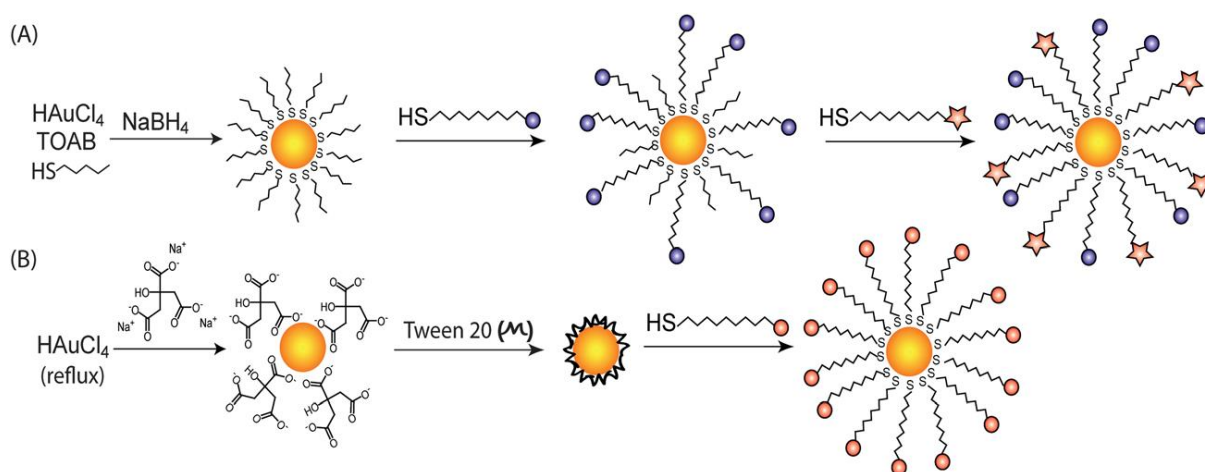


Figure 2.6. Gold nanoparticle stabilization (Daniel MC, Astruc D. (2014)).

## 2.2.2 Properties and applications of the AuNPs

The properties of AuNPs can be summarized on the following:

- **Biocompatibility and low toxicity**

It is really important to have reliable information on whether the AuNPs are toxic both isolated and being part of nanoconjugates.

Colloidal gold has a great chemical stability and therefore, it has been used historically on medical purposes. Consequently, it would be expected from gold nanoparticles to present a low toxicity and a big biocompatibility. Actually, according to Connor *et col.*, the gold nanoparticles cores are inert and non-toxic. Nevertheless, in recent bibliography discrepancy exist about its cytotoxicity, which could be related with the different sizes and shapes of the nanoparticles investigated and with the different agents utilized for its stabilization and functionality.

Pan *et al.* determined the effect of the nanoparticle size on the cytotoxicity of the AuNPs in different cellular lines. For this purpose, they used AuNPs soluble in water and stabilized with triphenylphosphine derivatives, with a size between 0.8 and 15 nm and they studied systematically its cytotoxicity on four representative cellular lines of the principal functional types: connective tissue fibroblasts, epithelial cells, macrophages and melanoma cells. They demonstrated that the answer and the cellular death mechanism depend on the size, being the AuNPs of 1.4nm on the different type of cells more sensible than de 15nm AuNPs.

It has been demonstrated that the superficial characteristics of the AuNPs have an influence on its toxicity. The cationic nanostructures present a higher toxicity than the anionic: anionic nanoparticles with a 2nm nucleus diameter are practically non-toxic whether the cationic equivalents are moderately toxic (probably related with the cellular lyses and the concentration).

- **Synthesis Ease**

AuNPs can be easily prepared, obtaining stable monodisperse colloidal systems with a size between 1 nm and 150 nm and a well-controlled size distribution.

The biography gathers different types of AuNPs, prepared using different techniques, which differ on the nanoparticles size, shape and physic properties. Some of the AuNPs shapes (Figure 2.7) are: nanospheres, nanocylinders, nanocovered, nanocages and “SERS”.

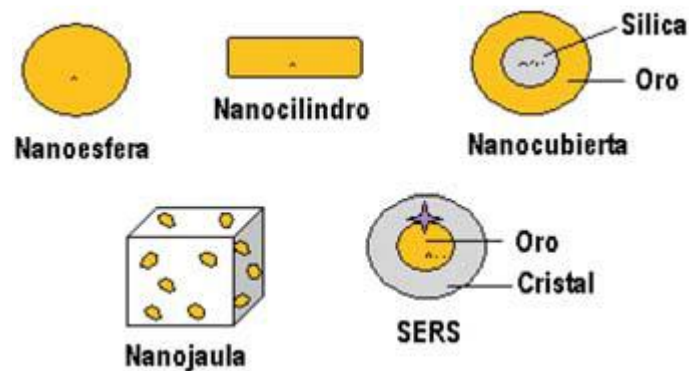


Figure 2.7. Different AuNPs shapes  
(<http://www.analesranf.com/index.php/mono/article/view/994/1028>)

The most utilized shape, gold nanospheres of 2-100 nm of diameter, can be obtained from the controlled reduction of gold chloride using different reducing agents and conditions. Faraday was the first one to prepare, in 1857, colloidal gold by reducing gold chloride with phosphorus, attributing its red color to the formation of really small particles. Years after, Mie corroborated that the colloidal gold color depends on the size. From then on, and especially during the last years, important efforts have been employed on the preparation via reduction of gold salts –generally using citrate as reducing agent and in presence of stabilizing agents that prevent agglomeration–, of AuNPs practically monodisperse and controlled size (ref.). It was confirmed that the relation citrate/gold and the velocity of addition of the reducing agent can affect the AuNPs size: when faster the addition of reducing agent is, smaller and more monodisperse the AuNPs become.

- **Multifunctionality**

AuNPs present a great superficial area, and therefore they can be easily functionalized and bioconjugated by modifying its superficial characteristics. A 2 nm AuNP could, theoretically, be conjugated to  $\sim 100$  molecules in available ligands ( $n = \sim 10^8$ ).

The AuNP functionalization is generally carried out via <<thiol>> connections, though they also show affinity for amino groups, phosphate and bisulfite. Many molecules have been linked to AuNPs surface for different purposes, opening its application field.

- **Photothermic properties**

In the nanometric scale, electromagnetic, optical and photothermal properties from noble metals are highly different from its corresponding properties on normal scale. For example, gold nanoparticles (AuNPs) have a reddish coloration while in its normal size is yellow.

The peculiarity of the optical and photothermal of the AuNPs are due to the resonant oscillations of its free electrons in presence of light(<<Resonance localize in the Plasmon surface>>), thanks to which the nanoparticles can irradiate light (Mie scattering) or absorb light which is transformed rapidly on heat. Indeed, AuNPs emit an intense heat when are stimulated with the correct frequency of light laser or another source of heat (microwaves, radiofrequency, ultrasounds...); thus, a collection of little AuNPs can heat locally an area of a thousand times its size, acting like <<nanoscopic heaters activated by the light>>.

This singular photothermic behavior its highly influentiated by its size, shape and surface properties, and that is the reason for which in the last years there has been a resurgence in the investigation on the synthesis and functionalization of AuNPs, in order to obtain nanoparticles with the optical characteristics for different purposes.

Some of the AuNPS different applications in biomedicine are:

- DNA-AuNPs Assemblies and sensors in the fields of biosensors, disease diagnosis and gene expression. (Mirking-Letsinger at Northwestern and Alvisatos-Schultz at Berkley investigation groups).
- AuNP-Enhanced immuno-sensing for the immunolabeling and imaging of cells, biomolecules and other biological components (Hayat in 1989).
- Transport of therapeutic agents to the cells in biomedical treatment (Stellacci *et al.*, 2011).
- Cancer treatment (Kotov *et al.*, 2008)

Gold nanoparticles can also be used in different catalysis.

### 2.2.3 Functionalized nanopapers with AuNPs

The last five years have witnessed fast progress in the field of microfluidic paper-based analytical devices ( $\mu$ -PADs), which represent new and outstanding approaches to simple, portable, disposable, and inexpensive devices for molecular analysis and monitoring health. Paper is a porous cellulose fiber web with large surface area, and the porous nature not only fulfills the primary tasks such as diagnostic tests using body fluids and fluid transport, but also makes it possible to pattern hydrophilic channels separated by hydrophobic walls of photoresist/polymer, inks, wax, or by plasma treatment, laser treatment and cutting method. In addition, these  $\mu$ -PADs can be well applied not only in point-of-care testing but also in field analysis in remote locations with limited facilities. Inspired by this simple technique, many groups have paid great efforts to the development of  $\mu$ -PADs, including fabrication methods for  $\mu$ -PADs, functionalizations for  $\mu$ -PADs, and analytical methods on  $\mu$ -PADs. The success of  $\mu$ -PADs arises from three main factors: low cost, ease of operation, and ability to function without any external pumps.

Although these  $\mu$ -PADs use paper as support to nanoparticles, there is no evidence that nanopaper has ever been used to be the matrix of these AuNPs. But as said before, nanopaper has different properties in comparison to ordinary paper due to the nanometric nature of its cellulose nanofibers. Therefore, the obtained nanopaper is

transparent and, when combined with AuNPs, the photothermic properties of these nanoparticles could be better used.

## 2.3 Surface Plasmon (SPs) and Surface Plasmon Resonance (SPR)

Surface plasmons (SPs) are coherent delocalized electron oscillations that exist at the interface between any two materials where the real part of the dielectric function changes sign across the interface (e.g. a metal-dielectric interface, such as a metal sheet in air). SPs have lower energy than bulk (or volume) plasmons which quantise the longitudinal electron oscillations about positive ion cores within the bulk of an electron gas (or plasma).

The charge motion in a surface plasmon always creates electromagnetic fields outside (as well as inside) the metal. The total excitation, including both the charge motion and associated electromagnetic field, is called either a surface plasmon polariton at a planar interface, or a localized surface plasmon for the closed surface of a small particle.

The ability to dynamically control the plasmonic properties of materials in these nano-devices is key to their development. A new approach that uses plasmon-plasmon interactions has been demonstrated recently. Here the bulk plasmon resonance is induced or suppressed to manipulate the propagation of light. This approach has been shown to have a high potential for nanoscale light manipulation and the development of a fully CMOS-compatible electro-optical plasmonic modulator, said to be a future key component in chip-scale photonic circuits.

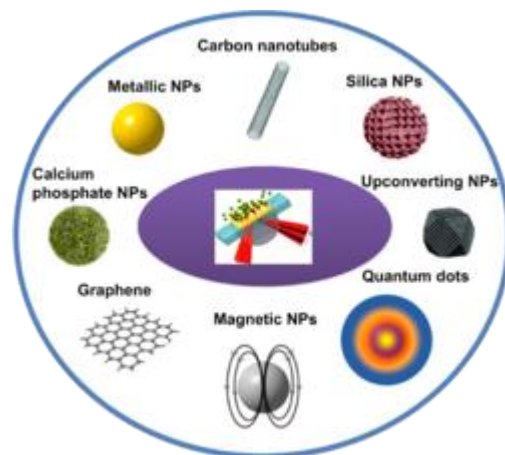


Figure 2.8. Nanomaterials enhanced SPR sensor  
([http://en.wikipedia.org/wiki/File:Nanomaterials\\_enhanced\\_SPR.png](http://en.wikipedia.org/wiki/File:Nanomaterials_enhanced_SPR.png))

To describe the existence and properties of surface plasmon polaritons, one can choose from various models (quantum theory, Drude model, etc.). The simplest way to approach the problem is to treat each material as a homogeneous continuum,

described by a frequency-dependent relative permittivity between the external medium and the surface. This quantity, hereafter referred to as the materials' "dielectric function," is complex permittivity. In order for the terms that describe the electronic surface plasmons to exist, the real part of the dielectric constant of the metal must be negative and its magnitude must be greater than that of the dielectric. This condition is met in the infrared-visible wavelength region for air/metal and water/metal interfaces (where the real dielectric constant of a metal is negative and that of air or water is positive).

The excitation of surface plasmons is frequently used in an experimental technique known as surface plasmon resonance (SPR). In SPR, the maximum excitation of surface plasmons are detected by monitoring the reflected power from a prism coupler as a function of incident angle or wavelength. This technique can be used to observe nanometer changes in thickness, density fluctuations, or molecular absorption.

Surface plasmon resonance (SPR) is the resonant oscillation of conduction electrons at the interface between a negative and positive permittivity material stimulated by incident light. The resonance condition is established when the frequency of incident photons matches the natural frequency of surface electrons scillating against the restoring force of positive nuclei. SPR in subwavelength scale nanostructures can bepolaritonic or plasmonic in nature.

The wavelength and intensity of the plasmon-related absorption and emission peaks are affected by molecular adsorption that can be used in molecular sensors. For example, a fully operational prototype device detecting casein in milk has been fabricated. The device is based on monitoring changes in plasmon-related absorption of light by a gold layer.

### 3. STATE OF THE ART

There are many publications and patents describing methods of attachment/binding of nanoparticles onto paper, particularly for TiO<sub>2</sub> functionalized paper (Garnier *et al.* 2011). And while the previous sentence is true, publications concerning nanopaper and gold nanoparticles seem nearly null over the five last years. Basically, there one approach for attaching nanoparticles onto paper, “wet-end addition”, where nanoparticles are adhered onto individual fibers before paper sheet formation, and “surface treatment”, where dry paper sheet is impregnated with nanoparticles by passing through a bath of chemicals which impregnates the paper surface or by coating.

Wet-end addition is more commonly used to prepare TiO<sub>2</sub> photocatalytic paper. Fukahori *et al.* and Iguchi *et al.* produced photocatalytic papers, which are made of TiO<sub>2</sub> supported by ceramic fibers, using the wet-end addition process. A TiO<sub>2</sub> containing paper of high stability was fabricated by preferential immobilization of photoactive TiO<sub>2</sub> nanoparticles onto the inorganic fibers, followed by incorporation into the layered pulp fiber network. This TiO<sub>2</sub> paper was made from beaten pulps and ceramic fibers according to Technical Association of the Pulp and Paper Industry (TAPPI) Test Methods T205.

Surface treatments are more promising than the wet-end addition, since nanoparticles can be concentrated near the paper surfaces. The extent of penetration of the nanoparticles into paper is controllable by the paper's hydrophobicity (sizing) and porosity (paper structure). There are different types of surface treatments, but we only intend to review the major existing methods to coat or impregnate nanoparticles onto paper, which are size press, layer-by-layer deposition (LbL), sol–gel method, direct assembly and in situ assembly.

Dry paper sheets are generally coated with a mixture of TiO<sub>2</sub> and different types of binder, to produce photocatalytic paper by using a size press in the papermaking process. There are several patents which incorporate different binders to coat TiO<sub>2</sub> onto paper substrates. For instance, colloidal silica used by Ahlstrom , resin binders

used by Eln Kohsan Co. and silicone binders used by Nippon Soda. These binders play an important role in immobilizing  $\text{TiO}_2$  onto paper and protecting the paper from photodegradation by  $\text{TiO}_2$  at the same time. Aguedach *et al.* and Railard *et al.* also coated paper with a mixture of  $\text{TiO}_2$  and colloidal silica using a size press. These studies highlighted the role of silica binder in increasing adsorption capacity of  $\text{TiO}_2$  to produce an efficient photocatalyst which is able to decompose textile dye in wastewater.

Pinto *et al.* also synthesized and deposited silica-coated AuNPs onto cellulosic fibers. This was the first time that cellulose was used as substrate for LbL assembly of AuNPs. The cellulose fibers were previously treated with polyelectrolytes to provide cationic charge by alternate dipping in poly(diallyldimethylammonium chloride) (polyDADMAC), poly(sodium 4-styrenesulfonate (PSS), and again in the polyDADMAC solutions (the basis of the layer-by-layer method). These treated cellulose fibers were then immersed in the Au colloids. The silica shells ensured that the individual Au cores were well separated, and prevented variation of plasmon oscillation frequency in the final assemblies. The adjustable optical properties, which can be obtained by modifying the surface of nanoparticles with silica shells, made these nanocomposites very attractive, particularly in the manufacture of security paper. Since it is important to prevent aggregation of AgNPs which will reduce their antimicrobial efficiency, this method could also be applied for AgNPs to develop antimicrobial paper, since the silica shells are able to maintain a good distribution of nanoparticles on the cellulose surface. However, diffusion of nanoparticles into the polyelectrolyte macromolecule should be further studied because this would reduce their contact with light and pollutants, thus decreasing their performance.

In direct assembly, AuNPs and AgNPs are usually synthesized by citrate reduction of aqueous Au and Ag salt solutions and then assembled onto paper. The citrate groups serve the dual role of reducing agent and stabilizer. They impart negative surface to nanoparticles from weakly bound citrate ions, which prevent agglomeration in solution and immobilize them on the substrates through electrostatic self-assembly. Dong and Hinstroza made cationic cellulose from cotton via grafting of positively charged ammonium ions for electrostatic deposition of AuNPs. The AuNPs are directly

assembled onto cellulose by immersing cationic cellulose into a citrate-reduced Au colloidal solution. Increasing concentration of the citrate enhanced negative surface potential of AuNPs and led to higher packing density of AuNPs on the substrate. Their procedure shows promise to allow deposition of other negatively charged metal nanoparticles onto cationically-modified cellulose substrates. Yet, the adsorption state of nanoparticles must be controlled to achieve a reproducible distribution, since it affects optical properties of the nanoparticles.

In another interesting approach, *Zhao et al.* synthesized DNA crosslinked AuNPs to produce a thermally-stable bioactive paper. Thiol-modified DNA was added to a citrate-reduced AuNP solution for DNA coupling. The blue colored DNA-cross-linked AuNP aggregates were then deposited on paper substrates. When endonuclease and adenosine were present, the bioactive paper degraded the crosslinked AuNP aggregates producing a deep red color. DNA crosslinked AuNPs were spotted on different types of paper substrates. Hydrophobic and (poly(vinyl alcohol)-coated) hydrophilic paper were found to be the best biosensor substrates, whereas untreated hydrophilic paper caused “bleeding” and precipitation resulting from surface drying. This work demonstrates the feasibility of functionalizing paper substrates with AuNPs to produce an effective, renewable and disposable bioactive paper. Nanoparticles can be dried on paper, heated and stored whilst still maintaining their aggregation/dispersion, as well as their activity upon subsequent exposure to target analytes.

*Cai et al.* performed another in situ formation of AuNPs in cellulose gel by physical reduction method. Transparent cellulose hydrogel films were immersed in a  $\text{HAuCl}_4$  solution, followed by heating at 80 °C for 24 h to achieve hydrothermal reduction. Highly dispersed and thermally-stable AuNPs were formed in the cellulose gels. The high porosity, near transparency and high mechanical strength of these AuNPs impregnated cellulose gels offer an attractive substrate for nanoparticle synthesis/support medium. This composite material is interesting for use in molecular detection via transmission UV–Vis spectroscopy. The presence of molecules will change the dielectric constant of the AuNPs and produce a shift in their absorbance

peak. However, distribution reproducibility of AuNPs within the cellulose gels needs to be addressed.

Although these many applications about cellulose and AuNPs, as said previously, there is only one publication in the last five years that has used nanopaper as a support for gold nanoparticles.

Takuya Kitaoka *et al.* used AuNPs as high-performance catalysts. In their work, gold nanoparticles (AuNPs) were considered among the most innovative catalysts, despite bulk Au metal being regarded as stable and inactive. The hybridization of metal NPs has attracted major interest in the field of advanced nanocatalysts, due to electro-mediated ligand effects. In practical terms, metal NPs need to be supported on a suitable matrix to avoid any undesirable aggregation; many researchers have reported the potential of polymer-supported AuNPs. However, the use of conventional polymer matrices make it difficult to take full advantage of the inherent properties of the metal NPs, since most of active NPs are imbedded inside the polymer support. This results in poor accessibility for the reactants. Herein, they reported the topochemical synthesis of Au and palladium (Pd) bimetallic NPs over the surfaces of 2,2,6,6-tetramethylpiperidine-1-oxyl (TEMPO)-oxidized cellulose nanofibers (TOCNs), and their exceptional catalytic performance. Highly-dispersed AuPdNPs were successfully synthesized in situ on the crystal surfaces of TOCNs with a very high density of carboxylate groups. The AuPdNPs@TOCN nanocomposites exhibit excellent catalytic efficiencies in the aqueous reduction of 4-nitrophenol to 4-aminophenol, depending on the molar ratios of Au and Pd.

Bimetallic NPs composed of Au and Pd were successfully synthesized on highly crystalline TOCN via high-densities of carboxylate on the surface in a facile one-pot reaction. AuPdNPs with varying molar ratios of Au and Pd were successfully immobilized and possibly exposed on the TOCN supports. The catalytic activity of AuNPs@TOCN was much higher than the support-free AuNPs and previously reported AuNPs-polymer composites. Furthermore, tailoring the Au and Pd molar ratios had

great influence on the catalytic activities for the reduction of 4-NP to 4-AP. In this study a molar ratio of 3:1 (Au:Pd) provided the best catalytic performance.

## 4. MATERIALS AND METHODS

### 4.1 Materials

On this section, the materials used on this project are described.

#### Gold nanoparticles

The gold nanoparticles were purchased from Sigma-Aldrich.

The AuNPs were stabilized in a suspension of citrate buffer in order to avoid aggregations. The solution has a reddish color. The particles had an average core size of 5 nm and a mean *hydrodynamic diameter*\* of 14-25 nm with an optical density (OD) of 1. In the following table, its specifications can be seen.

Formula:	Au
Formula Weight:	196.97 g/mol
Storage Temperature:	2 - 8 °C

TEST	Specification
Appearance (Form)	Suspension
Polydispersity Index (PDI)	< 0.2
Core Size	4 - 7 nm
Mean Hydrodynamic Diameter (Z)	14 - 25 nm
Particles/ml	Confirmed
4.92E+ 13-6.01E+ 13	
Absorption Max	510 - 525 nm
Concentration	Confirmed
(OD): 1	
Buffer	Confirmed
Stabilized suspension in citrate buffer	
Product of Supplier	Confirmed
CytoDiagnostics, Inc	

Figure 4.1. Purchased AuNPs properties  
(<http://www.sigmaaldrich.com/catalog/product/aldrich/741949?lang=es&region=ES>)

\*the hydrodynamic diameter is a parameter used to describe the aggregation diameter of the nanoparticles in solution.

---

Materials to obtain CNF:

**Dried bleached eucalyptus and pine pulp:** Commercial dried bleached eucalyptus pulp acquired from La Montañanesa, Grupo Torraspapel, Zaragoza, Spain is a pulp typically used by the papermaking industry for the fabrication of printing/writing paper. The Kappa number was 0.6, average viscosity 855.2 cm<sup>3</sup>/g and brightness 91.1%, according to the supplier. Previous to its use, the pulp was disintegrated in water with a laboratory pulper provided with a helicoidal rotor at 60000 revolutions. The resulting slurry was then filtered through a suitable fabric to eliminate the excess of water and retain only the wet fibers.

Materials for the TEMPO oxidation :

The reactants that are utilized for the oxidation are cited below. These are calculated on a base of 1 gram of dry pulp.

- **Sodium hypochlorite (NaClO):** is the oxidizing agent. Depending on the oxidation degree wanted, the quantity of NaClO added varies. It has a concentration of 2M.
- **TEMPO (2,2,6,6-Tetrametil-1-Piperidin-1-Oxil):** is the catalyst of the reaction.
- **Bromur de sodi Sodium bromide (NaBr):** it is added as for the hypochlorite to oxidase it to form sodium hypobromide (oxidase the TEMPO when it has oxidized the primary alcohol or the aldehyde of the fiber).
- **Sodium hydroxide (NaOH):** its function is to maintain the suspension at pH 10.

Materials to characterize CNF:

- a) Determination of carboxylic groups concentration following the conductimetry method:
- **Sodium chloride (NaCl):** it is added to improve the conductivity of the medium during the process of conductivity determination.
  - **Nitrogen gas:** it is used to avoid that the oxidation of the fibers due to the oxygen of the air.

- **Sodium hydroxide (NaOH)**: it is added to neutralize the acids and it has a concentration of 0,5 M.
- b) Determination of the cationic demand:
  - **PoliDADMAC (PoliDDA)**: it is a cationic polymer and its function is to be adsorbed in the CNF surface which are negatively charged.
  - **PES-Na**: anionic polymer, it is added to determine the PoliDDA that has not been absorbed in the CNF.

The two reactants are industrially standardized and have a concentration of 0.001N. Provided by BTG.

- c) Degree of polymerization determination.
  - **Copper (II) ethylenediamine (CED)**: is a solvent to dissolve the CNF, and therefore determine the properties of the cellulose in a solution.
  - **Copper pieces**: they are added into the solution in order to avoid the oxidation of the CED.

## 4.2 Methods

### 4.2.1 Pulp preparation

#### 4.2.1.1 Determination of the dryness

The determination of the humidity or of the dryness is performed in a fast and reliable way using a humidity analyzer, which has a heat resistance that evaporates the water and a balance with IR that measures the weight difference.

The analyzer used in this project is the one seen on Figure 4.2. This method is called thermogravimetry.



Figure 4.2. Thermobalance

The procedure followed is the following: get 2 grams approximately of pulp and put them in the thermobalance of the humidity analyzer. Before introducing the sample the balance must be zeroed and cold. Finally, we close the chamber and we wait for the constant weight of the sample.

The thermobalance gives the results in dry mass (%S) that are used in the calculus of the dry quantity of pulp to disintegrate.

### 4.2.1.2 Desintegration

To obtain the CNF the first step is to disintegrate the pulp. The aim of the process is to separate the fibers applying a mechanical work which does not affect its internal morphology. The methodology is followed from the ISO 5263.

The process consists on weighting approximately 30 dry grams and leave them with water at 20°C minimum during 4 hours. After that, we break the paper into little pieces and we introduce them into the pulper (Figure 4.3. Pulper). When the process is finished, we get the pulp and we filter it in a vacuum. After that it can be kept hermetically in a refrigerator between 3 and 5°C.

The pulper has a control system that allows to control the spinning velocity of the rotor, the time, the energetic consume and the temperature of the suspension.



Figure 4.3. Pulper

### 4.2.2 Consistency

When the pulp is already filtered, the consistency is determined as to use in posterior calculus. This determination follows the UNE-57-020.

To calculate the consistency of a sample is necessary to know the humid weight (initial weight). A certain quantity of humid pulp is introduced in the oven at 105°C until it loses

all the humidity, in other words, until constant weight. The sample is removed from the oven and is left in the desiccator until it accomplishes room temperature. Finally, the sample is weighted (this will be the dry weight).

The calculus is the following (eq.1):

$$\% \text{ consistency} = \frac{\text{dry weight}}{\text{wet weight}} \times 100 \quad \text{eq. 1}$$

### 4.2.3 Obtention of CNF

The obtention of CNF is explained on the following steps:

- a. Refine the pulp mechanically at 4000 revolutions.
- b. Oxidize the pulp using the TEMPO reaction.
- c. Pass the resulting pulp through the homogenizer and obtain the CNF gel.

#### 4.2.3.1 Mechanical refine PFI

The procedure of mechanical refine follows the ISO 5264-2. The instrument of refine PFI has two different parts: the refine grinding and the cylindrical container. The refine grind has 33 knives and spins at 1440 rpm, while the cylindrical container spins at 720 rpm at the same direction.

The instrument has a control panel where the revolutions needed to refine the pulp can be programmed, as well as the working time and the consumed energy in order to achieve the needed revolutions. Following the ISO, it is worked with a maximum of 30 grams of dry pulp with a consistency of 10%, and therefore, the suspension that is introduced in the stator will be maximum 300 grams.

To precede to the refining, the suspension of pulp is introduced in the cylindrical container, it is distributed uniformly on its lateral wall and the needed revolutions are programmed. Finally, the refining grinder is lowered and the security lid is closed.

To begin the refine, the instrument is started and the lever is lifted. This lever will release a weight that will apply a pressure of 3.33kN over the pulp during the test. The pulp makes that no physical contact between the knives from the grinder and the container wall happens.

When the instrument achieves the selected revolutions it returns to the initial state, the refined pulp is extracted and the grinder is cleaned. At this point, the sample is defibrillated and ready to oxidize.



Figure 4.4. PFI equipment

#### 4.2.3.2 TEMPO-mediated oxidation

The objective of the TEMPO reaction is to oxidize the primary alcohol of the cellulose chain to an additional carboxylic acid adding a determined quantity of NaClO. Depending on the quantity of NaClO added we can obtain new degrees of oxidation. First of all, it is necessary to calculate the quantity of reagents, explained on the materials section, that are needed for a certain quantity of dry pulp. In the following table, it can be seen the quantity of reagents needed for the TEMPO oxidation per gramm of dry pulp.

The wanted oxidation state is determined to calculate the quantity of oxidant agent (NaClO) needed to be added.

After that, a beaker with the adequate capacity is prepared to obtain a pulp of consistency 1,5% and the quantity of water is added. For example, if we want to oxidize 15 g of pulp with a consistency of 1,5% a volume of 1500 mL is needed.

Afterwards, the TEMPO and the NaBr reactants are added and stirred until a complete dissolution with the water. Finally, the pulp is added and the solution is stirred until a complete homogenization. Normally, a smooth mechanical agitation is sufficient.

The reaction medium is highened at pH 10 with the solution of NaOH which has a known concentration of 0,5 M. And, drop by drop, the solution of NaClO is added maintaining the pH at 10. When the volume of necessary NaClO is finished, NaOH is added at the solution until the pH of the solution is has a constant value of 10 (the reaction medium has to be basic all the time).

When the pH is constant, the agitation is stopped, the solution is filtered and the remaining pulp is washed several times in order to eliminate the remaining NaOH.

#### **4.2.3.3 Homogenizing of the CNF**

The homogenizer shown in the Figure 4.5, is the instrument that is used to obtain the gel-like CNF. This instrument works at high-pressure, until 2000 bars. The solution gets in as a aqueous suspension with a consistency between 1 and 2 %, and gets out in a gel-like form after few passes at 600 bars.

When the solution passes through a reduced diameter at high pressure a fibrillation of the oxidized fibers is produced and that increases the tendency to form new hydrogen

bonds with the water in the medium. When these bonds are formed, the water absorption capacity of the fibers is heightened as well as its specific surface area.

Experimentally, a sample with a consistency of 1-2% is prepared in order to obtain the



**Figure 4.5. Homogenizer**

optimal work conditions to homogenize. After that, the vessel of the homogenizer is filled and another vessel is placed on the way out tube. Depending on the oxidation state of the fibers, more or less passes are needed to obtain CNF with good efficiency. When the CNF gel-like substance is obtained, the homogenizer must be cleaned with distilled water.

The following step is to characterize the CNF gel-like substance.

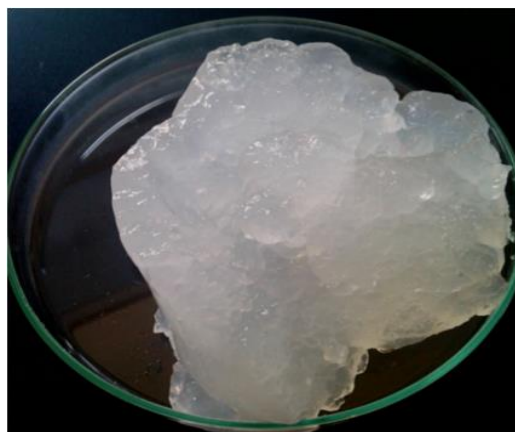


**Figure 4.6. CNF gel-like substance**

## 4.2.4 CNF characterization

The parameters of consistency, yield of fibrillation, carboxylic groups concentration, polymerization degree, WRV and cationic demand are characterized of the 4 types of CNF that have been prepared (Pine 10 and 15 and Eucalyptus 10 and 15).

### 4.2.4.1 Consistency

When the CNF are obtained the first characterization done is the consistency determination as it is needed to do any calculus involving these nanofibers. Basically, the quantity of solids in the gel-like suspension of nanofibers is determined. The procedure is the same as for the dryness determination because the CNF have a high-quantity of water.

An exact quantity of CNF is weighted in an already tared watch glass and it's put into the oven at a temperature of 100-105°C until it reaches a constant weight. When the sample is dry, we introduce it in the desiccator as for it to reach room temperature. After that, it is weighted and the dry weight is obtained. The consistency is calculated using eq. 1 (section 4.2.2)

### 4.2.4.2 Yield of fibrillation

The determination of the efficiency consists on knowing the quantity of initial fiber that has been unstructured and converted on CNF. This determination can be made following two methods, the direct method or the centrifugation and the determination of the transmittance.

#### 4.2.4.2.1 Centrifugation method

This method consists on preparing 150 mL of a solution of 0,1% of CNF. This calculation is easier using the following equation:

$$P_{NFC} = \frac{C_{solution} \times V_{solution}}{C_{NFC}} \quad eq. 2$$

Where,  $P_{NFC}$  is the weight in grams of wet CNF that has to be weighted,  $C_{solution}$  the desired consistency in %, which is 0.1%,  $V_{solution}$  is the volume of the solution in mL and CNF is the consistency of the CNF in percentage.

The sample is centrifuged during 30 minutes at 10000 rpm to separate the CNF from the supernatant of the non fibrillated fibers that sediment. After that, the supernatant liquid is decanted and the sediment fraction is dried until constant weight in an oven at 105°C. The centrifugal machine use can be seen in Figure 4.7.

The efficiency ( $\eta$ ) of the CNF fraction in percentage is calculated with this formula:

$$\eta (\%) = \left(1 - \frac{P_{SS}}{P_{SM} \times C_{CNF}}\right) \times 100 \quad eq. 3$$

Where,  $P_{SS}$  is the weight of the dry sediment in grams,  $P_{SM}$  is the weight of the wet sediment in grams and  $C_{CNF}$  is the consistency of the prepared CNF in percentage.

It is necessary that the value of the efficiency is higher than 80 % to consider a good oxidation of the fibres. If the efficiency is lower, than 80%, that indicates that the oxidation hasn't correctly taken place and it might be repeated.



Figure 4.7. Centrifugation equipment

#### 4.2.4.2.2 Transmittance

The transmittance is a spectrophotometric method that used to determine the efficiency of the CNF. This method consists on measuring the transmittance of a solution at 0,1% of CNF using the spectrophotometer of Figure 4.8.



Figure 4.8. Spectrophotometer

To perform this method, 50 mL of a well-homogenized CNF solution at 0,1% might be prepared. Afterwards, the transmittance of this solution is measured. To measure it, a screening at 800nm using mili-Q water as blank is performed.

#### 4.2.4.3 Carboxylic content

This determination is a very important characterization because it will be the diferencial criteria of the CNF. Its objective is to determine the present quantity in mmol of carboxylic acid per grams of cellulose of pulp that have been previously oxidized before homogenizing.

#### 4.2.4.3.1 Conductimetry method

This method is the most reliable to determine the mmols of carboxylic acid presented per gram of cellulose of oxidized pulp. It consists on measuring the conductivity of a sample of CNF with a conductivity-meter (Figure 4.9).

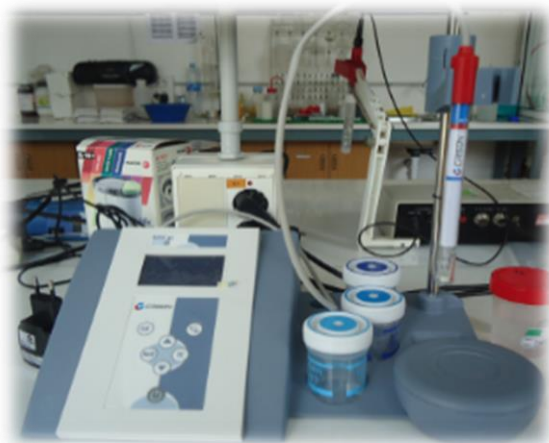


Figure 4.9. Conductivity-meter

To perform a correct analysis, the procedure is the following:

0,3 grams of dry pulp are weighted and added at a mixture of 55 mL of distilled water and 5 mL of a solution of 0,01 M NaCl. After that, the sample is stirred for 20 minutes to achieve a homogenous mixture. Before analyzing the sample, the conductivity meter and the pH meter must be calibrated; after that, we proceed with the sample. Following that, nitrogen gas is bubbled into the sample and its pH is adjusted between 2,5 and 3 using a dilution of 0,01 M HCl. This solution is titrated with a standardized solution of NaOH with a concentration of 0,05M. 0,1 mL of NaOH are added, at the beginning of the titration, and we should wait until the conductivity meter value is constant and note this value down. This procedure is repeated until the pH is 8 or higher. After that we represent the obtained values in a graphic plotting the added NaOH with the conductivity.

As it can be seen on the graphic (Figure 4.10) that the slope 2 is the zone where the conductivity is constant, which means, when the carboxylic acid is converted in carboxylate. To determine this conductivity, the slopes 1 and 3 are obtained. After that,

these slopes are equalized to the constant value of conductivity of the slope 2 in order to determine  $V_1$  (the volume used in the slope 1) and  $V_3$  (the volume used in the slope 3). The difference between these two volumes is the volume of NaOH necessary to neutralize all the carboxylic acids of the pulp. This can be seen on the following equation:

$$COOH \left( \frac{mmol}{gr} \right) = \frac{(V_3 - V_1) \times C_{NaOH}}{W} \quad eq. 4$$

where,  $C_{NaOH}$  is the exact concentration of NaOH and  $W$  is the dry weight in grams of the sample.

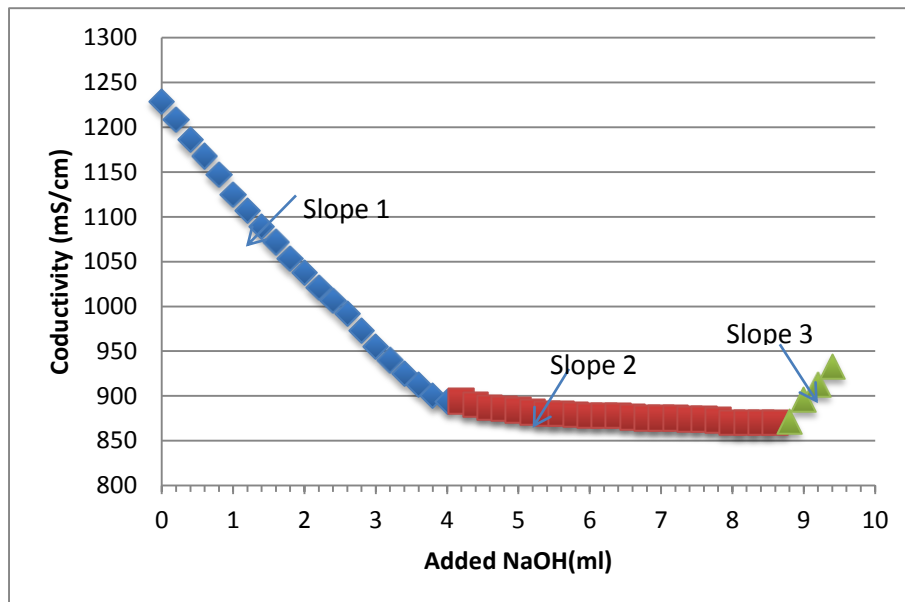


Figure 4.10. Change of the conductivity in the carboxylic content determination

#### 4.2.4.4 Cationic demand

The cationic demand of a sample gives information about the quantity of the charges cationic polymer which is necessary to neutralize the superficial load of the particulates in the sample. This determination, of liquid samples, is done using a Müttek instrument, like the one seen in Figure 4.11.

First of all, 40 mg of wet CNF are weighted, therefore, the dry weight of the sample must be calculated using the consistency. These wet CNF are diluted with 1 L of distilled water and are dispersed with a pulp disintegrator during 10 min at 3000 revolutions. After that, 10 mL of the solution are added to 25 mL of PoliDADMAC and are magnetically stirred during 5 minutes.

Following that, the mixture is centrifuged during 30 minutes at 10000 rpm to separate the two phases. 10 mL of the supernatant are taken and analyzed with the Mütek. A titration of the PoliDADMAC with PES-Na is performed, adding reduced volumes of this last reagent with a micropipette, until arriving at a 0 mV value.



Figure 4.11. Mütek

As a recommendation of the instrument manufacturer, the maximal volume that has to be used to consider the test correct is 6,25 mL, as for higher volumes the instrument loses accuracy. If the value is higher, the test should be repeated using less quantity of dry weight of quantity. The calculus is made by the following equation:

$$Demanda\ catiónica\left(\frac{\mu eq}{gr}\right) = \frac{(6,25 - V)}{pes\ sec} \quad eq. 5$$

Where  $V$  corresponds to the volume of PES-Na in mL that are used as to reach the value of 0 mV.

#### 4.2.4.5 Degree of polymerization

The degree of polymerization is determined by measuring the intrinsic viscosity of the pulp after the TEMPO oxidation and before the homogenizing, as the homogenizer lowers drastically the degree of polymerization and what interests us is the effect of the oxidation on the pulp. This procedure follows the UNE 54-039-92.

The assay is done using an Ostwald viscometer submerged in a water bath as to have a constant temperature of 25°C. This can be seen on Figure 4.12. Solutions of different concentrations from the same sample are prepared (60, 80, 125 and 200 mg/L). This should be prepared in 50 mL of distilled water.



Figure 4.12. Ostwald viscosimeter

After that, 25 mL of CED are treated with amide groups and filtered to eliminate the copper dust before adding into the previous solution, putting 3 pieces of copper to prevent the oxidation of the CED. We put the mixture in magnetic stirring until a perfectly homogenous solution is obtained. After that, we fill the bulb of the Ostwald

viscometer and we note down the time needed for the solution to go from one line to the other. Three measurements per sample are needed for a correct average value.

A measure from the blank sample is also determined, as it is the time that the CED dilutions without the pulp needs to cover the same distance as the samples. This time ( $t_0$ ) makes it able to calculate the relative viscosity ( $\mu_r$ ), the specific viscosity ( $\mu_{esp}$ ), the inherent viscosity ( $\mu_{inhe}$ ) and also the reduced specific viscosity ( $\mu_{red}$ ). The calculation for all of this values is done using the following equations:

$$\mu_r = \frac{t}{t_0} \quad Eq.6$$

$$\mu_{esp} = \frac{(t - t_0)}{t_0} \quad Eq.7$$

$$\mu_{inhe} = \frac{\ln(\mu_r)}{C} \quad Eq.8$$

$$\mu_{red} = \frac{\mu_{esp}}{C} \quad Eq.9$$

Where,  $t$  i  $t_0$  are the terms of the oxidized pulp and the blank and  $C$  is the concentration of the used solutions.

In the case of the inherent and reduced viscosity, the measurement units are dL/g.

The intersection of the evolution corresponding with the inherent viscosity and the reduced specific viscosity against the curves of concentration corresponds with the intrinsic viscosity ( $\mu$ ) of the sample. The intrinsic viscosity is related with the degree of polymerization (DP) with the equation 10:

$$\mu = k \times GP^\alpha \quad Eq.10$$

$$\ln\mu = \ln k + \alpha \times \ln GP \quad Eq.11$$

Where the terms of the equation  $k$  and  $\alpha$  are the coefficients that depend on the temperature, polymer and the solvent. To eliminate the concentration and the interaction of the near chains it is necessary to extrapolate the intrinsic viscosity at a concentration equal to 0 ( $C=0$ ), using the linearized equation 10 (eq. 11).

#### 4.2.5 Nanopaper formation and characterization

As said previously, the nanopaper we have formed has different characteristics. They were formed via casting in PP Petri dishes of about 9 cm of diameter. Regardless of its oxidation state or its source (pine or eucalyptus), its formation procedure is the same.

First of all, the quantity of necessary CNF for the wanted grammage is calculated. After that, the calculated weight of CNF gel-substance is introduced into a 100 mL beaker. Distilled water is poured in the beaker until the 50 mL is reached. After that, we use the Ultraturrax to make a homogenous liquid. As the mixture has gotten air bubbles and it is not completely homogenized, the following step will be the use of the sonicator. Apart from that, if we need to add a certain quantity of gold nanoparticles, it will be between these two steps that will be poured into the CNF mixture. While the Ultraturrax will be used for approximately a minute, the sonicator will be used for minimum 2 minutes as to obtain a sample without bubbles.

When all the air bubbles are removed from the sample, we can proceed to the formation of the nanopaper. This formation is called "Casting" and it is based on the natural water evaporation. It consists on pouring the sample into a Petri dish and first of all, putting the sample during 24h into an oven at 50°C and after that, let the remaining water evaporate via putting the samples into a fume hood until we obtain the transparent nanopaper. Once we see that the sample is dry, we can remove the nanopaper from the Petri dish; this last step is the more difficult one, as we have to be very cautious not to break the sample when separating it from the Petri dish.

### 4.2.5.1 Thickness

The determination of the thickness of the paper follows the ISO 534-2011.

On the Figure 4.13 the used micrometer is shown. For the correct use of the equipment, the instrument is placed in a rigid surface in order to avoid the vibrations that could vary the different thickness readings.

First of all, the instrument is zeroed and the desired paper is introduced between the charge and the surface. After that, the charge is downed and the value of the thickness in mm is noted.



Figure 4.13. Micrometer

### 4.2.5.2 FE-SEM microphotography

FE-SEM is the abbreviation of the word Field Emission Scanning Electron Microscope. Scanning and electron transmission microscopes (SEM and TEM) use as a source for image formation electrons (particles with a negative charge), in contrast to light microscopes (LM). These electrons are produced by a Field emission source in a FE-SEM. The sample (object) is scanned in a kind of zig-zag pattern by an electron beam.

A FE-SEM is used to visualize very small topographic details on the surface or entire or fractioned objects.

Researchers in biology, chemistry and physics apply this technique to observe structures that may be as small as 1 nanometer (= billion of a millimeter). The FE-SEM may be employed for example to study cell organelles and DNA material, synthetic polymers, and coatings on microchips.

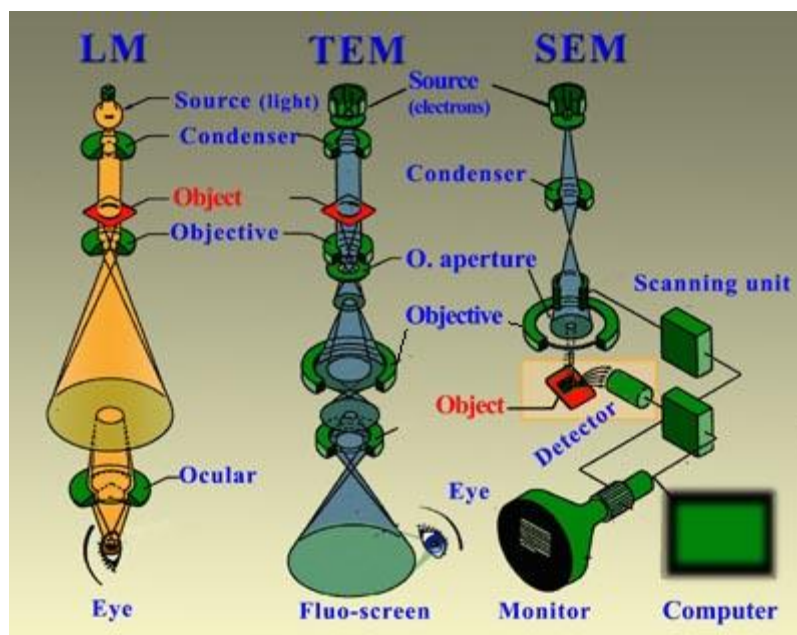


Figure 4.14. FE-SEM equipment scheme  
(<http://www.vcbio.science.ru.nl/en/FE-SEM/info/fesemfaq/>)

In our case we the FE-SEM microphotographys were carried out by the research technical services (STR) of the University of Girona.

#### 4.2.5.3 Transmittance

The same procedure as the explained on section 4.2.4.2.2 is followed.

#### 4.2.5.4 Mechanical properties

Three mechanical properties are going to be studied: tensile strength, Young's modulus and strain at break.

Tensile index describes the tensile strength of paper in relation to the amount of material being loaded. This parameter differs from the usual engineering definition of stress, which is force per unit cross-section of the test specimen. This difference arose historically because of the difficulty of accurately measuring the thickness of paper sheets. Another way of expressing the tensile strength of paper is in terms of breaking length by dividing tensile strength by grammage. Strength at break is the calculated upper limit of length of a uniform paper strip that would support its own weight if it were suspended at one end. Tensile index and strength at break mainly depend on the degree of fiber bonding, fiber strength and fiber length and is usually studied to determine the capability of bonding between fibers. Finally, the Young's modulus, also known as the tensile modulus or elastic modulus, is a measure of the stiffness of an elastic material and is a quantity used to characterize materials.

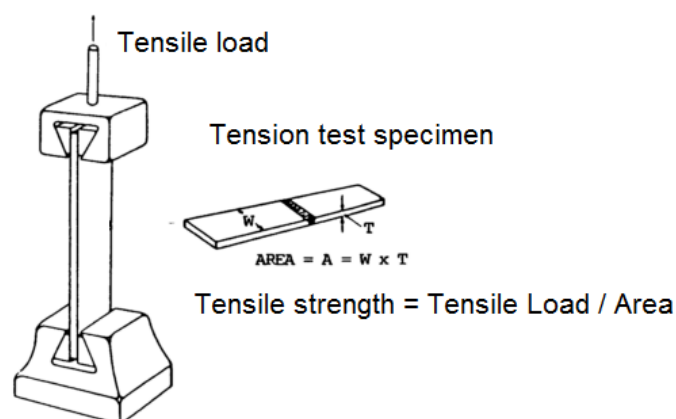


Figure 4.15. Tensile strength test specimen and test method (<http://www.angelfire.com/my/welding/test.html>).

Paper samples were mechanically tested in an Instron universal testing machine provided with 250 N load cell. The testing specimens were cut down to stripes of 40 mm length and 10 mm width. In order to calculate tensile strength and Young's modulus, the thickness of the testing samples was determined with a micrometer, measuring 5 different zones of the strip and calculating the average.

The used equipment was a Hounsfield Instron dynamometer.

To begin the assay, the sample is placed in the middle of the two clamps. The clamps have a coarse surface that prevents the paper from slip, therefore, the results of tensile strength can be more reliable.



Figure 4.16. Hounsfield Instron dynamometer

Apart from the dynamometer, a computer is needed as for installing the software that gives information of FMax, MYoung, AFMax, CMax, etc.

#### 4.2.5.5 Surface Plasmon resonance determination

LSPRs (Localized SPRs) are collective electron charge oscillations in metallic nanoparticles that are excited by light. They exhibit enhanced near-field amplitude at the resonance wavelength. This field is highly localized at the nanoparticle and decays rapidly away from the nanoparticle/dielectric interface into the dielectric background, though far-field scattering by the particle is also enhanced by the resonance. Light intensity enhancement is a very important aspect of LSPRs and localization means the LSPR has very high spatial resolution (subwavelength), limited only by the size of nanoparticles. Because of the enhanced field amplitude, effects that depend on the amplitude such as magneto-optical effect are also enhanced by LSPRs.

The Kretschmann-Raether configuration is mostly employed for the excitation of surface plasmons (SPs) in thin films. Figure 4.17 displays a scheme of the home-made surface plasmon resonance (SPR) device designed and mounted in the Departamento de Electrocerámica at the Instituto de Cerámica y Vidrio (CSIC) of Madrid, showing the different elements of the experimental setup. Figure 4.17 shows a picture of the system.

In this geometry, SPs are excited in the attenuated total reflectance mode using a HeNe (632.8 nm) linearly polarized laser. The laser is mounted on a cradle equipped with yaw and pitch movements for an accurate orientation of the beam on the sample. A linear polarizer is used to have a p-polarization. Subsequently, a beam splitter detects the laser intensity to a photodetector, in order to record fluctuations in laser intensity during the experiments. Beyond the beam splitter, the laser beam is modulated with an optical chopper, working at 479 Hz. Finally, the laser light reaches the sample. The sample consists of a thin metallic film (typically 50 nm of Au or Ag, using in this work Au films) grown on a glass substrate. The sample is fixed to the prism through the substrate side using gel index matching for a good coupling. Both (sample and prism) are mounted on top of a rotating motor that allows varying the laser incidence angle.

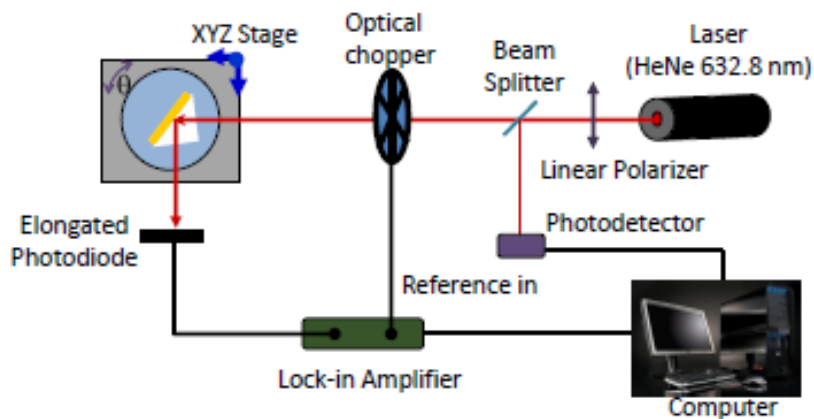


Figure 4.17. Scheme of a Kretschmann-Raether SPR device

Surface Plasmon resonance has only been performed with the more transparent samples which are pine 10 and 15 mmol as for a good measurement of SPR a high transparency is required.

## 5. RESULTS AND DISCUSSION

On this section, this project's experimental results and their discussion are going to be presented. First of all, the results of the characterization of the different types of used CNF are going to be presented. After that, the physical, optical and mechanical characterization results of both nanopaper and nanopaper/AuNPs composites are going to be explained.

### 5.1 CNF characterization

The characterization of the CNF is an essential task, provided that gives information of the efficiency of the production procedures and the properties of these CNF. The studied parameters are the consistency, the yield of fibrillation, the carboxylic groups' content, the cationic demand and the degree of polymerization.

#### 5.1.1 Consistency

The consistency of the obtained nanofibers is shown in Table 5.1.

Table 5.1. Consistency values

Nanopaper type	Consistency (%)
Pine 10 mmol	1,01
Pine 15 mmol	0,77
Eucalyptus 10 mmol	1,72
Eucalyptus 15 mmol	1,15

With these results of consistency we can make all the calculations to fabricate the nanopaper as we know the percentage of nanofibers on the CNF gel-like obtained substance.

#### 5.1.2 Yield of fibrillation

The yield of fibrillation is very important as it is characteristic of the fibrillation degree of each CNF type. This determination is made with the oxidized pulp, after it has been

passed through the homogenizer. This assay can be performed, as said previously, following two methodologies: centrifugation and transmittance.

### 5.1.2.1 Centrifugation method

In this project, the maximum CNF yield of fibrillation has been tried to achieve. For that reason, first of all, the number of passes of the suspension through the homogenizer to obtain a compact gel-like substance with a high fibrillation degree is needed to know. On the Table 5.2 we can see the results.

The centrifugation does not give information about the exact value of the yield of fibrillation because when the CNF have a high efficiency no precipitated solids are found in the recipient. For that reason, a precise result cannot be obtained. As highest result, we can say that the efficiency is above 95%. Therefore, this method is not a reliable one. For that reason, we also use the transmittance method that can provide more exact results. At the Table 5.2 it can also be seen that the more oxidized the CNF are, less passes through the homogenizer they need to achieve a high efficiency and a compact gel-like texture. This fact has a logic explanation as when a higher oxidation degree of the CNF is achieved, more negatively charged are in the surface which permits the liberation of the nanofibers during the homogenization.

Table 5.2. CNF yield of fibrillation via centrifugation method

Nanopaper type	Yield of fibrillation (%)	Homogenizer passes
Pine 10 mmol	>95	3
Pine 15 mmol	>95	2
Eucalyptus 10 mmol	>95	4
Eucalyptus 15 mmol	>95	2

### 5.1.2.2 Transmittance

Transmittance is another method to determine the yield of fibrillation of the CNF. At a wavelength of 800nm the transmittance value is the maximum, and therefore it can be used as an indirect reference to know the fibrillation degree of the CNF. In Table 5.3

the values of the transmittance are shown and it can be seen that with a higher oxidation degree, lower is the number of passes through the homogenizer to obtain a higher value of transmittance. Mili-Q water is used as reference.

**Table 5.3. CNF transmittance**

<b>Nanopaper type</b>	<b>Transmittance (%) at 800nm</b>
Pine 10 mmol	98,4
Pine 15 mmol	99,4
Eucalyptus 10 mmol	82,8
Eucalyptus 15 mmol	84,7

This assay indicates the presence of bigger-sized nanofibrilated material in the sample as a simple nanofiber has a diameter of 5-7 nm, which does not scatter the light, and therefore the transmission would be 100%. On our case, though, it could be seen that the light is slightly scattered and therefore we can conclude that aggregates with a diameter of over 400 nm must exist in order to have a lower transmittance of 100%.

### 5.1.3 Carboxylic group content

#### 5.1.3.1 Conductimetry titration

This method is the most reliable and direct one to determine the carboxylic group rate of each type of CNF. The obtained values are in Table 5.4.

**Table 5.4. Carboxylic group rate**

<b>Nanopaper type</b>	<b>Carboxylic group (<math>\mu\text{eq/g}</math>)</b>
Pine 10 mmol	982
Pine 15 mmol	1145
Eucalyptus 10 mmol	1197
Eucalyptus 15 mmol	1326

As it has been commented before, during the oxidation of the fibers using NaClO, the hydroxyl groups are converted in aldehyde and carboxylic groups. This fact is directly

related with the carboxylic groups rate as when more oxidized the fibers are, more hydroxyl groups would have converted to carboxylic groups. So as expected, it is seen that while the oxidation state increases so does the COOH rate but, at the same time, there might be a determined oxidation degree where the COOH rate remains constant.

#### 5.1.4 Cationic demand

Generally, the cationic demand is a parameter that indicates the evolution of the specific surface of the pulp with the mechanical refine. The values of the cationic demand from the different CNF types are shown in Table 5.5.

Table 5.5. Cationic demand

Nanopaper type	Cathionic demand ( $\mu\text{eq/g}$ )
Pine 10 mmol	1657
Pine 15 mmol	1838
Eucalyptus 10 mmol	1783
Eucalyptus 15 mmol	1988

As more oxidized the fibers are, more negatively charged is its surface and therefore, more volume of cationic polymer is needed to neutralize them. The carboxyl groups have the property to transfer to the medium the hydrogen from the hydroxyl group and remain negatively charged. Therefore, the more carboxylic groups there are, more negatively charged is the surface of de CNF.

#### 5.1.5 Degree of polymerization

The initial degree of polymerization (DP) of the used cellulose fibers wasn't determined, but it is known that this value is between 300 and 1700, and therefore a mean of 1000 units (*Shinoda, Saito et al. 2012*). The polymerization degree has different values as it changes depending on the cellulose origin, and the fiber pretreatment.

The oxidation process of the fibers causes a depolymerization of the amorphous zones of the cellulose chains. There are two types of depolymerization for the cellulose, the first is the  $\beta$ -elimination caused by the aldehyde groups formed in the C-6, as the intermediate structure under alkali conditions. The other type is the rupture of the glycosidic bounds of the cellulose chain caused by the active hydroxyl radicals and other species formed in situ during the TEMPO reaction. In the Table 5.6 the results of the degree of polymerization (DP) are shown.

**Table 5.6. Degree of polymerization**

<b>Nanopaper type</b>	<b>DP</b>
<b>Pine 10 mmol</b>	237
<b>Pine 15 mmol</b>	170
<b>Eucalyptus 10 mmol</b>	229
<b>Eucalyptus 15 mmol</b>	197

During the oxidation process, started and controlled by the addition of NaClO, the cellulose polymerization degree is highly affected. As it can be seen with the values, with the increase of added NaClO in the reaction, higher is its effect and the breaking of the chains, and therefore lower is the degree of polymerization.

## 5.2 Nanopaper characterization

### 5.2.1 Morphology

Following the procedure explained in section 4.2.5.1 the results of thickness for the obtained nanopapers are the following (Table 5.7):

Table 5.7. Thickness results

Nanopaper type	Thickness (mm)
Pine 10 mmol	0,022
Pine 15 mmol	0,019
Eucalyptus 10 mmol	0,022
Eucalyptus 15 mmol	0,02

It could be seen that the thickness decreases as the oxidation of the used fibers rises. That can be explained as when the carboxylic content increases, the CNF are more individualized and their average diameters smaller so fibers can pack closely together and therefore the thickness of nanopapers diminish. Also, for CNF oxidized with 15 mmol of NaClO, those obtained from pine pulps tend to be thinner than their eucalyptus counterparts; this is due to the greater individualization (smaller diameter) of the pine nanofibers and which permits to obtain thinner nanopapers.

FE-SEM microphotographs of nanopapers, showed that cellulose nanofibers were distributed in layers. Cellulose nanofibers are held together mainly by hydrogen bonds; the number of hydrogen bonds will depend on the fibrillation degree of the CNF suspension. The increase in the number of hydrogen bonds is the main parameter that affects the physical and mechanical properties of nanopapers and of papers in general. CNF in nanopapers are expected to distribute randomly within the structure.

FE-SEM microphotographs of nanopapers are presented on Figure 5.1.

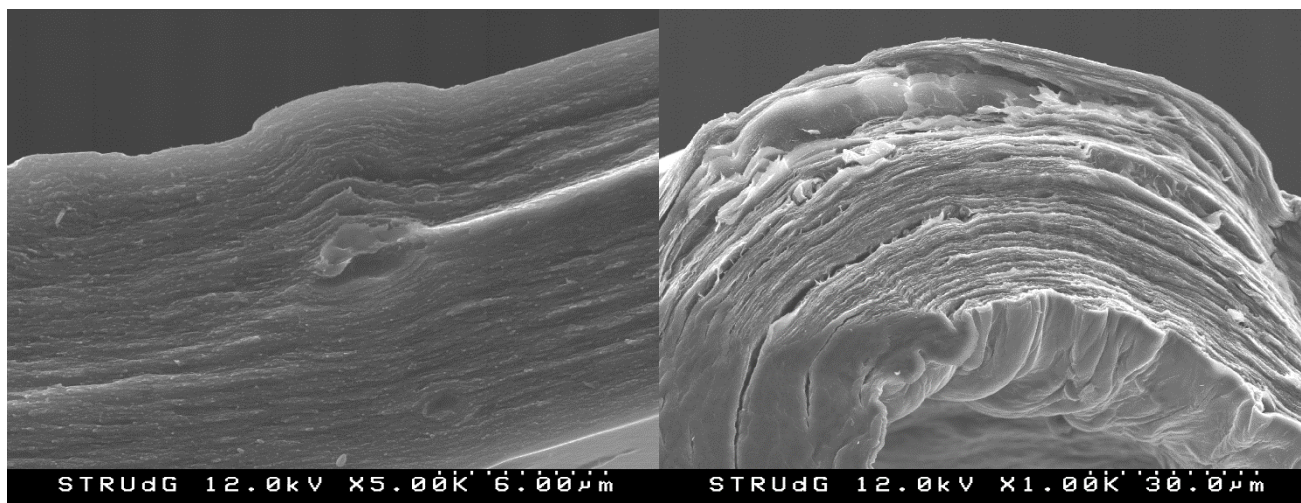


Figure 5.1. Microphotographs of nanopapers

## 5.2.2 Transmittance

The transmittance parameter, determined with a spectrophotometer showed some differences between the nanopapers. The different obtained graphs are shown on Figure 5.2.

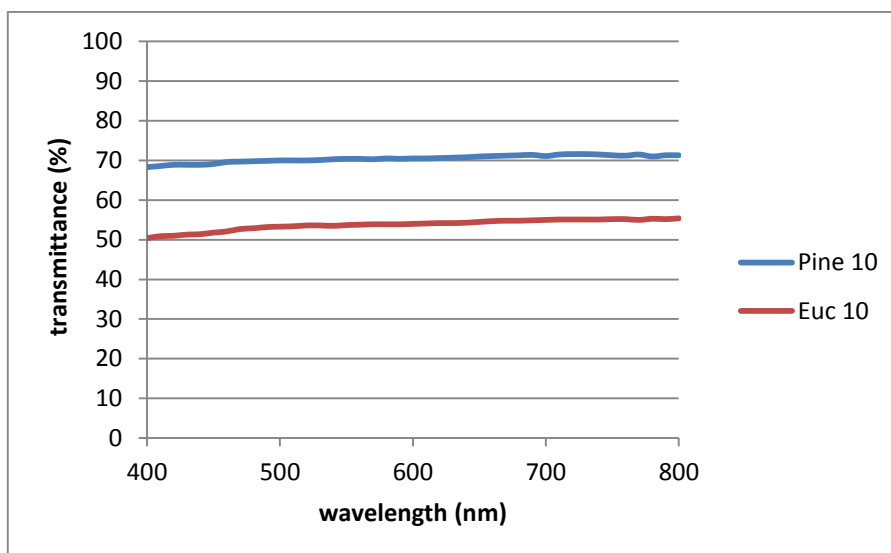


Figure 5.2. Transmittance of 10 mmol oxidized fibres

In both cases it could be seen that nanopapers made out of pine fibers had a better transmittance than the eucalyptus ones. This is due to the highest degree of fibrillation achieved by CNF from pine in comparison to eucalyptus.

Apart from that, the more oxidized the fibers are, the more transparent they are. If we talk about pine, its transmittance was around 70 % if the oxidation is 10 mmol of NaClO and around 85% with 15 mmol. The same was seen with eucalyptus nanopapers. A 10 mmol oxidized nanopaper has a transmittance of 52% and a 15 mmol oxidized nanopaper has a 75 % of transmittance at 800 nm wavelength.

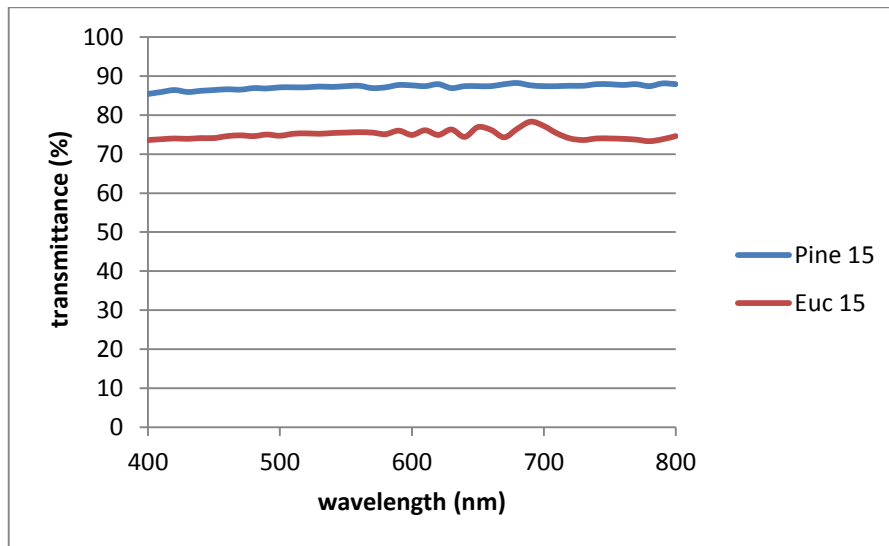


Figure 5.3. Transmittance of 15 mmol oxidized fibres

### 5.2.3 Mechanical properties

Tensile strength, Young's modulus and the strain at break of nanopapers were determined. The results are shown in Table 5.8:

**Table 5.8. Mechanical results**

Sample	Tensile strength	Young's modulus	Strain at break
	(MPa)	(GPa)	(%)
Pine 10 mmol (P10)	153,97±23,63	16,073±0,60	1,76±0,51
Eucalyptus 10 mmol (E10)	103,97±13,64	11,890±2,75	1,45±0,40
Pine 15 mmol (P15)	154,58±23,59	21,121±2,14	3,03±1,31
Eucalyptus 15 mmol (E15)	129,86±10,31	15,483±1,05	1,52±0,25

The results showed that pine nanopaper had a higher tensile strength than the eucalyptus one. Its value is around 150 MPa and its standard deviation is for both, P10 and P15, around 20 MPa. With E10 the mean of tensile strength is 103,97 MPa and with E15 is 129,86, being both values lower than pine nanopaper. Its standard deviation is lower than the one of pine nanopaper being around 13 MPa for E10 and around 10 for E15. These results can be explained if we take a look to the chemical results (CNF characterization) previously obtained. Pine nanofibers had higher transmittance results which translate into more individualized fibers. This boosts the formation of hydrogen bonds which is the main mechanism that rules the increase in mechanical properties of cellulose papers and nanopapers. This fact also leads to more compact, less porous structures that evenly distribute mechanical load and therefore with induce higher tensile strength.

If the results of Young's modulus and strain at break are now compared, it will be seen that P15 oxidized nanopaper has better results than E10 oxidized one. It can also be seen that although with the tensile strength values pine and eucalyptus nanopapers differed considerably Young's modulus and strain at break values are all quite similar except for the results of P15. In the case of these nanopapers, the Young's Modulus values are considerably higher (21 GPa) and so do the strain at break values (3%).

### 5.2.4 Surface Plasmon resonance

In the obtained graph (Figure 2.2) using the SPR equipment, we cannot see any peak. That is normal, as with a transparent, neat nanopaper no interaction with any sample exists.

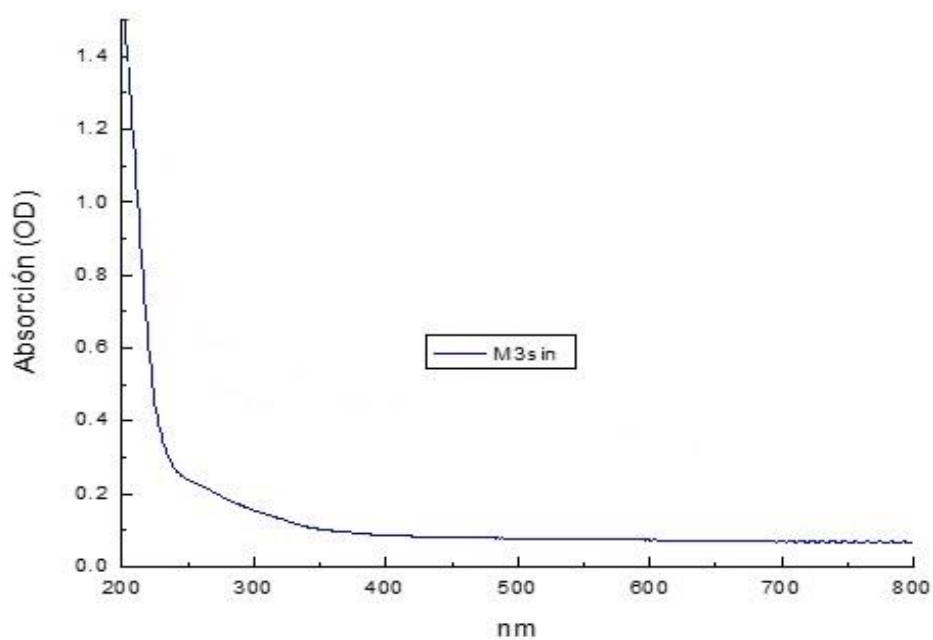


Figure 5.4. SPR of a Pine 15 mmol nanopaper

## 5.3 AuNP/nanopaper composite characterization

### 5.3.1 Morphology

In Table 5.9 the results of the thickness assays performed on the samples that contain gold nanoparticles (AuNPs) can be seen.

**Table 5.9. Thickness determination**

<b>Nanopaper type</b>	<b>Thickness (mm)</b>
Pine 10 mmol	0,022
Pine 10 mmol + 1,5 mL Au	0,022
Pine 10 mmol + 3 mL Au	0,024
Pine 15	0,019
Pine 15 mmol + 1,5 mL Au	0,019
Pine 15 mmol + 3 mL Au	0,018
Eucalyptus 10	0,022
Eucalyptus 10 mmol + 1,5 mL Au	0,023
Eucalyptus 10 mmol + 3 mL Au	0,02
Eucalyptus 15	0,02
Eucalyptus 15 mmol + 1,5 mL Au	0,019
Eucalyptus 15 mmol + 3 mL Au	0,02

Samples from 10 mmol nanopapers, whether they have more or less quantity of gold nanoparticles, have a higher thickness than the more oxidized fibers (15mmol); this has been explained before, as more oxidized nanofibers tend to be better packed.

If now the thickness of the nanopaper without AuNPs and the samples with AuNPs is compared, it can be seen that the values are similar. Also, with these results it cannot be extracted that more or less gold nanoparticles make the thickness vary. So in conclusion, the integration of AuNPs in a nanopaper matrix does not greatly vary its thickness.

On this FE-SEM microphotography (Figure 5.5) can be seen how the gold nanoparticles are distributed within the fibers. We can also measure the diameter of

the nanoparticles using the scale. If this diameter is measured, it can be seen that the AuNPs have a diameter from 25 to 50 nm which coincides with the hydrodynamic diameter (Z) given by the providers information. There are AuNPs that seem bigger and in those cases, we can assume that this might be an aggregation. Generally, though, we can see that AuNPs are well-dispersed within the nanopaper.

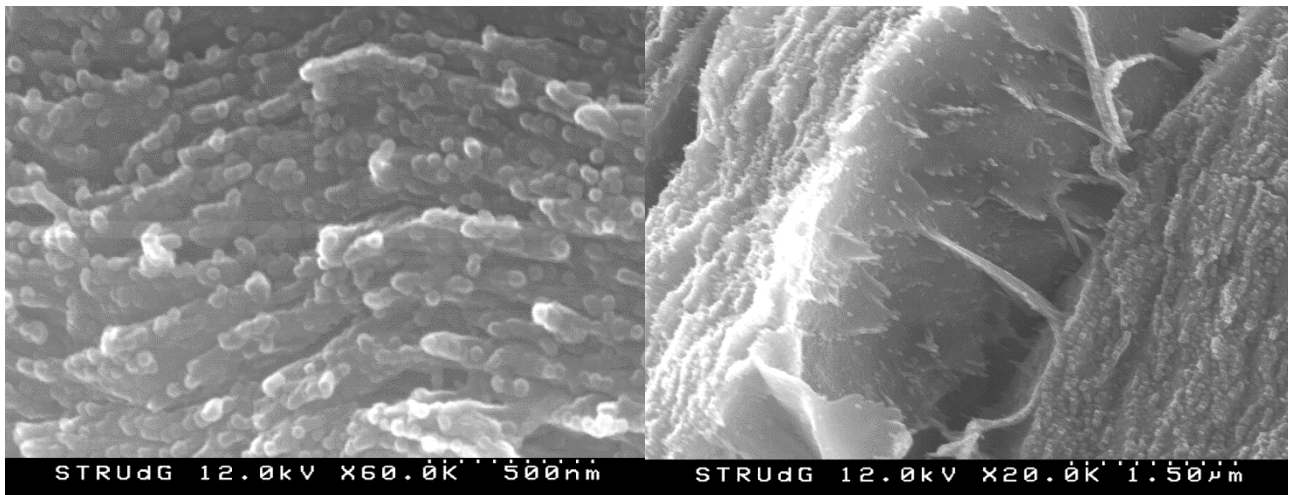


Figure 5.5. FE-SEM of AuNPs integrated into a nanopaper

### 5.3.2 Transmittance

The transmittance of AuNPs/CNF nanopapers from fibers oxidized with 10 and 15 mmol of NaClO is represented in Figure 5.6 and Figure 5.7. In general, the addition of AuNPs reduced nanopapers transmittance in comparison with their neat counterparts.

If we gather the nanopapers with the same quantity of gold nanoparticles it can be seen that the more oxidized nanopapers are, they have a higher percentage of transmittance than the less oxidized ones and that the pine-fiber nanopapers are always more transparent than the eucalyptus ones.

As expected, nanopapers with the same quantity of gold nanoparticles (1,5 mL) as more oxidized this nanopaper was, a higher percentage of transmittance had. It could

also be observed, that pine-fiber nanopapers were always more transparent than the eucalyptus ones.

In nanopapers with 3 mL of AuNPs the transmittance was lower and between the different types of nanopapers the differences were reduced. Again, P15 and E15 had higher transmittance than P10 and E10 with the same quantity of AuNPs. With this quantity of gold, it could be observed that a peak tendency began to appear between 500 and 600 nm where the red-band is (remember that gold nanoparticles have a reddish color). It could also be seen that when the quantity of AuNPs in the composite increases, the transmittance decreases in the pine nanopapers whether in the eucalyptus ones they tend to the same value.

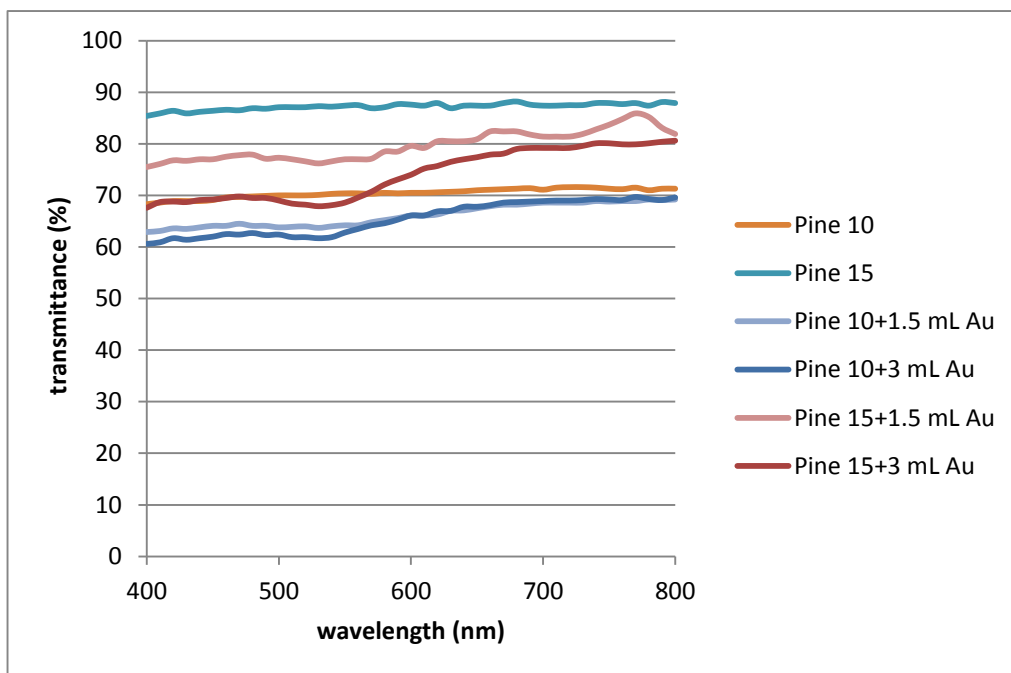


Figure 5.6. Transmittance of the pine nanopapers

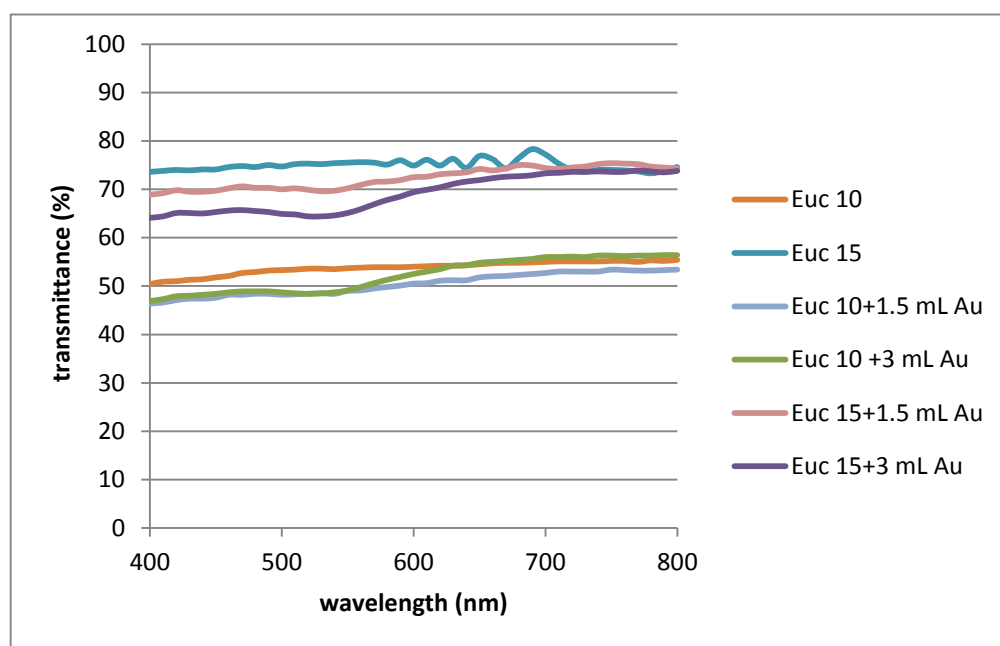


Figure 5.7. Transmittance of the eucalyptus nanopapers

### 5.3.3 Mechanical properties

Table 5.10 shows the results of the different mechanical determinations studied.

In general, it can be said that CNF with high carboxylic content renders nanopapers with better mechanical properties. The addition of gold nanoparticles decreased the overall tensile strength of nanopapers from pine pulps in comparison to neat samples and the most significant decrease was found in samples with 3 mL of AuNPs. Pine 15 with 1,5 ml of AuNPs has a lower value than E15 with the same quantity of gold, whereas the same nanopaper with 3 mL of AuNPs had the opposite results.

With pine nanopapers (with 1,5 and 3 mL of AuNPs) oxidized with 10 mmol of NaClO have better tensile strength than their corresponding eucalyptus counterparts.

The Young's modulus presented the most significant decrease in samples from pine pulps, in particular those oxidized with 15 mmol of NaClO. Interestingly, nanopapers from eucalyptus pulps did not show important changes in stiffness. The higher Young

modulus value found in AuNPs/nanopaper was for the eucalyptus 10 with 3 mL of AuNPs and lower one, as said, is the pine 15 with 3 mL of AuNPs.

Another important feature observed was that, in general, the addition of AuNPs did not modify the strain at break of nanopapers, regardless of the type of pulp or carboxylic content. The values of strain at break are all between 1,14 and 1,72 except for those commented previously: Pine 15 with 1,5 mL of AuNPs has a value 3,61% and Pine 15 with 3 mL of AuNPS has a value of 4,6%.

**Table 5.10. Mechanical results**

Sample	Tensile strength	Young's modulus	Strain at break
	(MPa)	(GPa)	(%)
Pine 10 mmol	153,97±23,63	16,073±0,60	1,76±0,51
Pine 10 mmol + 1,5 mL Au	112,9±16,03	12,281±1,33	1,72±0,55
Pine 10 mmol + 3 mL Au	91,993±23,06	11,987±3,68	1,21±0,50
Pine 15 mmol	154,58±23,59	21,121±2,14	3,03±1,31
Pine 15 mmol + 1,5 mL Au	139,203±21,46	8,651±1,63	3,61±1,18
Pine 15 mmol + 3 mL Au	144,64±34,50	7,66±3,52	4,16±1,30
Eucalyptus 10 mmol	117,61±13,64	14,64±2,75	1,45±0,40
Eucalyptus 10 mmol + 1,5 mL Au	111,153±7,36	13,96±1,77	1,51±0,43
Eucalyptus 10 mmol + 3 mL Au	101,98±17,81	13,87±1,74	1,14±0,25
Eucalyptus 15 mmol	140,17±10,31	15,483±1,05	1,52±0,25
Eucalyptus 15 mmol + 1,5 mL Au	149,24±11,82	16,18±2,22	1,7±0,18
Eucalyptus 15 mmol + 3 mL Au	120,356±19,08	15,86±1,79	1,6±,027

Generally, it can be seen the mechanical properties of nanopapers that contain gold nanoparticles tended to be poorer than the ones from neat nanopaper. This fact is due to the presence of gold as, even being well-dispersed in the nanopaper, it makes that the force applied during the tensile experiment was not equally distributed in all the nanofibers within the nanopaper. The tendency did not shown huge decreasing of the properties.

### 5.3.4 Surface plasmon resonance

It can be observed on Figure 5.8 that the excitation of surface Plasmons of the gold nanoparticles in the nanopaper had taken place. In the graph of the left side, the curves of the neat nanopaper alongside with the nanopapers added with 1.5 mL and 3 mL of AuNPs can be seen.

A higher absorption occurs when the quantity of AuNPs is increased. In the right figure where the curves have been subtracted from the blank we can clearly see that the peaks are located between 500-600 nm which is the band where the red is represented.

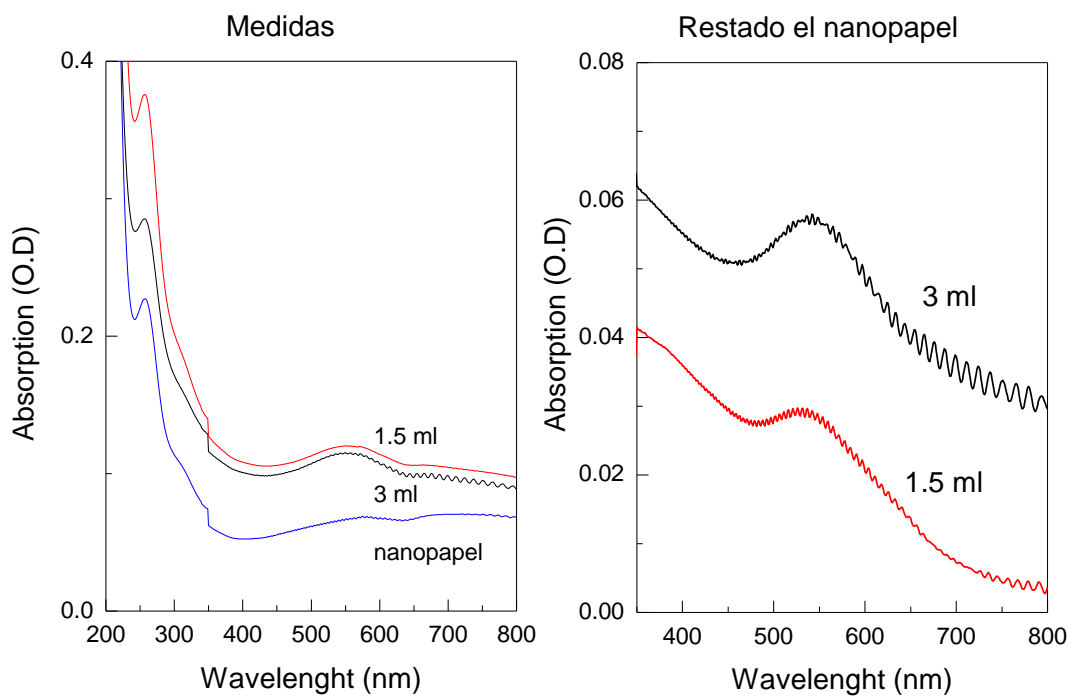


Figure 5.8. Surface Plasmon resonance results

In Figure 5.8 we see that the peaks of both P15+1,5 mL and P15+3 mL have the same area. To study how the surface Plasmon resonance evolved with the quantity of added gold, we analyzed two more samples, one with 6 mL of AuNPs and the other with 9 mL.

As it can be observed in Figure 5.9, with the addition of more AuNPs the peak increased from height and area, which meant that the SPR had excited the Plasmon of those nanoparticles.

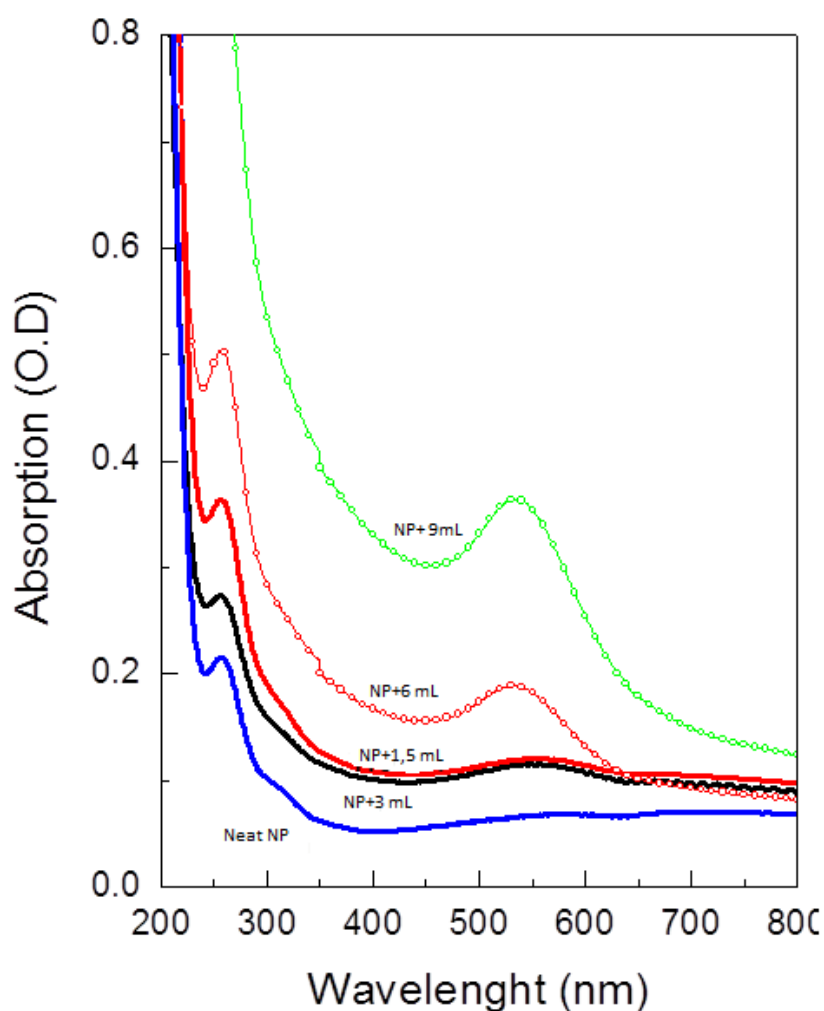


Figure 5.9. Surface Plasmon resonance results

The oscillations observed in the plots were produced by interferences due to nanopaper's thickness. The higher content of AuNPs in the sample produced a more intense peak at the aforementioned wavelength. The absorption of a neat nanopaper was also plotted along with those of AuNPs-added samples in order to show the increase clearly. The principles of AuNPs-enhanced SPR is due to the strong field coupling between localized SPR (LSPR) of AuNPs and SPR of the sensing film. Besides, it has been also reported that AuNPs size influences the signal response in a way that enhanced SPR sensing signals decrease with increasing particle size, mainly due to the fact that the influence of scattering in AuNPs with large diameters (>40 nm) becomes much stronger than the absorption (Zeng, S., *et al.*, 2013).

## 6. CONCLUSIONS

In the present work, CNF were produced via the TEMPO oxidizing method at an alkaline pH and room temperature. A total of 4 different types of nanofibers were produced: Pine 10 mmol, Pine 15 mmol, Eucalyptus 10 mmol and Eucalyptus 15 mmol. All this nanofibers were characterized analyzing its consistency, yield of fibrillation, carboxylic content, cationic demand and degree of polymerization. The results showed that a higher amount of COOH groups reduces the degree of polymerization, and at the same time the cationic demand increased and the transmittance is high at 800 nm. Also, the carboxylic content influences the number of passes through the homogenizer, reducing them while the carboxylic content increases.

These nanofibers were used to make nanopaper. These nanopapers were circular and were calculated to have a grammage of 30 g/m<sup>2</sup> and an area of approximately 75 cm<sup>2</sup>. The method of formation of these nanopapers was via casting. This method has the advantage of being really simple, easy to prepare and performed at room temperature with water as its solvent. Twelve types of nanopapers were formed: P10, P10+ 1,5 mL, P10 +3 mL, P15, P15 + 1,5 mL, P15 +3 mL, E10, E10 + 1,5 mL, E 10 +3 mL, E15, E15 + 1,5 mL and E15 +3 mL. The characterizing assays on nanopapers were: the thickness, the transmittance, the FE-SEM microscopy, the mechanical properties and the surface plasmon resonance.

Pine nanopapers, were more transparent, and therefore had a higher transmittance than the homologues eucalyptus-based nanopapers. This fact was due to the difference of diameter of the two types of nanofibers; Pine nanofibers are more individualized and therefore, when forming, the nanopapers are more compacted and form more bonds within the nanopaper structure. When AuNPs were added, transmittance decreased slightly. We could also see that when we added the highest quantity of AuNPs, a peak at 550nm was formed, this was due to the color of the AuNPs, which is red. In case of the eucalyptus nanopapers the tendency was nearly the same as with the pine nanopapers. E15 nanopapers also had higher transmittance

percentages than E10 nanopapers, although as said previously, these values were lower than the homologous pine nanopapers.

When talking about the thickness, it could be observed that when more quantity of AuNPs were added, the thickness did not tend to vary a lot, which means that this added quantity of AuNPs did not affect the nanopaper thickness which could induce to think that the nanoparticles are well dispersed in the material.

With the FE-SEM microscopy we could see how the fibers are distributed to form the nanopaper and if the AuNPs are well distributed on the material. It could also be seen that the nanofibers were distributed in layers to form the nanopaper and that the gold nanoparticles were well-dispersed within the nanopaper. Using the scale of the microscopy we could also observe that the diameter of the nanoparticles is not the core diameter provided by Sigma-Aldrich but a bigger diameter, from 25 to 50 nm, that corresponds with the mean hydrodynamic diameter (Z).

The mechanical assays showed that the presence of AuNPs in the nanopaper slightly worsened the mechanical properties in comparison to neat nanopaper. An explanation could be that the strength applied in the assays doesn't distribute equally on all the material due to the presence of AuNPs and therefore provoking tensions which make the material more vulnerable to tensile strength. Although it could be thought that the values of this parameter, Young's modulus and strain at break would diminish a lot when adding more quantity of AuNPs, it could be seen that the results did not have a drastic decrease. This fact makes us conclude that the addition of AuNPs in a material like nanopaper does not affect greatly on its mechanical properties.

Finally, it could be observed that the nanopaper containing 1,5 mL or more AuNPs acquires plasmon resonance properties. This means that in the different field where AuNPs are applied, these nanopapers containing AuNPs could be functionalized and could serve, for example, medical purposes.

To conclude, we would say that we have achieved a nanopaper/AuNPs composite which had enough AuNPs to be active (shown in the SPR) and which has a high transparence (which would mean a higher interaction with light and therefore an easier activation of the AuNPs). We have seen that AuNPs induce discreet reduction in mechanical properties. This new composite could be applied in fields like biomedicine if these nanoparticles are functionalized.

## 7. COSTS ESTIMATION

All the costs that have supported the investigation of this final project are detailed in this section.

To carry out this project, an investment in equipment and some material has to be made. In the following table all the equipment used is mention as well as its initial value ( $V_i$ ), its final value ( $V_f$ ) and the amortization that corresponds to a useful life of 10 years.

The final value ( $V_f$ ) represents the value of the equipment's after its useful life has passed, which we consider is 10 years. In this project the final value represents a 15% of the initial value. And therefore:

$$\text{Final value (Vf)} = \text{initial value (Vi)} \times 0,15 \quad \text{eq. 12}$$

To calculate the annual amortization we can follow this equation:

$$\text{Annual amortization} = \frac{\text{initial value(Vi)} - \text{final value(Vf)}}{\text{useful life}} \quad \text{eq. 13}$$

Table 7.1. Investment on equipment

CNF OBTENTION			
EQUIPMENT NAME	Initial value (€)	Final value (€)	Annual amortization(€)
PFI	36.000	5.400	3.060
pH-metre	100	15	8,5
Homogenizer	20.000	3.000	1700
CNF CHARACTERIZATION			
Centrifugal machine	9672	1.450,80	822,12
Spectrophotometer	12.000	1.800,00	1020
Mütek	11.638	1.745,70	989,23
Viscometer	100	15,00	8,5
Bath (viscometer)	1.154,99	173,25	98,17415
Conductivity-meter	100	15,00	8,5

<b>NANOPAPER OBTENTION AND CHARACTERIZATION</b>			
Refrigerator	1.000	150	85
Ultraturrax	3.000	450	255
Sonicator	8.000	1200	680
Mechanical agitator	1.200	180	102
Thermobalance	490	73,5	41,65
Oven	1.500	225	127,5
Dissecator	255	38,25	21,675
Precision balance	2.000	300	170
Micrometer	950	142,5	80,75
Hounsfield	7.000	1050	595
<b>TOTAL</b>			<b>9.873,60</b>

On Table 7.2, the prices of the used reactants of for this project have been quantified.

**Table 7.2. Reactant prices**

<b>Reactant name</b>	<b>price €/unit</b>	<b>unit</b>	<b>Total price (€)</b>
Bleached Eucalyptus	0	1	0
Bleached Pine	0	1	0
Cationic Starch	0	1	0
Gold nanoparticles (in a citrate buffer)	272	1	272
Sodium hypochloride (NaClO)	20,19	2	40,38
TEMPO	220	1	220
Sodium Bromide (NaBr)	109,39	1	109,39
Sodium Hydroxide (NaOH)	90,83	6	544,98
Methylene Blue	124,94	2	249,88
Sodium borate (Na <sub>2</sub> B <sub>4</sub> O <sub>7</sub> )	86,82	3	260,46
Chlorhydric acid (HCl)	32,04	2	64,08
Sodium Chloride (NaCl)	17,4	2	34,8
PoliDADMAC	169	3	507
PES-Na	169	3	507
Copper (II) ethylenediamine (CED)	81,2	1	81,2
Copper pieces	0	12	0
Destillated water	0,3	18	5,4
Mili-Q water	0,5	5	2,5
<b>TOTAL</b>			<b>2.899,07</b>

On the following table, the results of the costs of labor for each operation are detailed.

**Table 7.3. Labour costs**

<b>LEARNING AND WRITING THE PROJECT</b>			
Assay name	Time (h)	Price (€/h)	Total
Learning about the methods	35	0	0
Bibliographic research	40	25	1000
Analysis of the results	90	25	2250
Document redaction	150	25	3750
<b>OBTENTION AND CHARACTERIZATION OF THE CNF</b>			
Mechanical Refine (PFI)	2	10	20
TEMPO reaction	30	30	900
CNF homogenizing	25	20	500
Consistency and yield of fibrillation	10	20	200
Carboxylic groups determination	30	20	600
Cationic demand	10	20	200
Polymerization degree	15	20	300
<b>OBTENTION AND CHARACTERIZATION OF THE NANOPAPER</b>			
Nanopaper formation	80	20	1600
Thickness	3	10	30
Density	4	10	40
Transmittance	2	10	20
FE-SEM microscopy	4	30	120
Mechanical properties	10	20	200
Surface Plasmon resonance	8	50	400
<b>TOTAL</b>	<b>548</b>	<b>365</b>	<b>12.130</b>

Finally, a final value of the estimation cost for the project is obtained. In Table 7.4 and Figure 7.1, we can see these values and how are they distributed.

Table 7.4. Total costs estimation

Category	Price (€)
SUBTOTAL	12.130
INDIRECT COSTS*	1.820
AMMORTIZATION COSTS	9.873,60
REACTANTS COST	2.899,07
<b>TOTAL COST ESTIMATION</b>	<b>26.722,17</b>

*\*The indirect costs are referred to the electricity and water use. To calculate their value we consider that they represent a 15% of the cost of labor.*

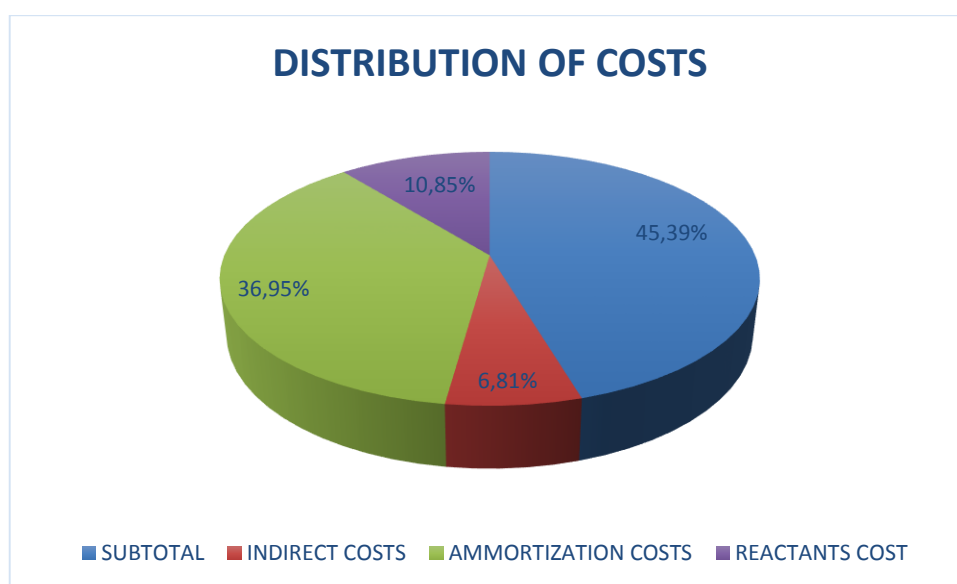


Figure 7.1. Distribuiton of costs

## 8. EVOLUTION OF THE PROJECT: GANTT DIAGRAM

Activity	2014	2015					
	12	1	2	3	4	5	6
Discussion and choosing of the project							
Bibliographic research							
"Full de projecte" writing and hand over							
Nanofibers obtention and characterization							
Nanopaper formation							
Nanopaper assays and characterization							
Nanopaper + AuNPs tests							
Nanopaper + AuNPs characterization							
Analysis of the results							
Writing of the project							
Writing of the synopsis							

## 9. BIBLIOGRAPHY

Beck-Candanedo, S., M. Roman and D. G. Gray (2005). "Effect of reaction conditions on the properties and behavior of wood cellulose nanocrystal suspensions." Biomacromolecules 6(2): 1048-1054.

Besbes, I., S. Alila and S. Boufi (2011). "Nanofibrillated cellulose from TEMPO-oxidized eucalyptus fibres: Effect of the carboxyl content." Carbohydrate Polymers 84(3): 975-983.

Chauhan, V. S. and S. K. Chakrabarti (2012). "USE OF NANOTECHNOLOGY FOR HIGH PERFORMANCE CELLULOSIC AND PAPERMAKING PRODUCTS." Cellulose Chemistry and Technology 46(5-6): 389-400.

Chinga-Carrasco, G. (2011). "Cellulose fibres, nanofibrils and microfibrils: The morphological sequence of MFC components from a plant physiology and fibre technology point of view." Nanoscale Research Letters 6: 7.

Fukuzumi, H., T. Saito, T. Wata, Y. Kumamoto and A. Isogai (2009). "Transparent and High Gas Barrier Films of Cellulose Nanofibers Prepared by TEMPO-Mediated Oxidation." Biomacromolecules 10(1): 162-165.

Hubbe, M. A., O. J. Rojas, L. A. Lucia and M. Sain (2008). "Cellulosic nanocomposites: a review." BioResources 3(3): 929-980.

Isogai, A. (2013). "Wood nanocelluloses: fundamentals and applications as new bio-based nanomaterials." Journal of Wood Science 59(6): 449-459.

Isogai, A., T. Saito and H. Fukuzumi (2011). "TEMPO-oxidized cellulose nanofibers." Nanoscale 3(1): 71-85.

Klemm, D., F. Kramer, S. Moritz, T. Lindström, M. Ankerfors, D. Gray and A. Dorris (2011). "Nanocelluloses: A New Family of Nature-Based Materials." Angewandte Chemie International Edition 50(24): 5438-5466.

Kulachenko, A., T. Denoyelle, S. Galland and S. B. Lindström (2012). "Elastic properties of cellulose nanopaper." Cellulose 19(3): 793-807.

Lojewski, T., K. Zieba and J. Lojewska (2010). "Size exclusion chromatography and viscometry in paper degradation studies. New Mark-Houwink coefficients for cellulose in cupri-ethylenediamine." Journal of Chromatography A 1217(42): 6462-6468.

Nogi, M., S. Iwamoto, A. N. Nakagaito and H. Yano (2009). "Optically transparent nanofiber paper." Advanced Materials 21(16): 1595-1598.

Potulski, D. C. (2013). "Efeito da incorporação de microfibrilas de celulose sobre as propriedades do papel."

Qua, E., P. Hornsby, H. Sharma and G. Lyons (2011). "Preparation and characterisation of cellulose nanofibres." Journal of materials science 46(18): 6029-6045.

Saito, T. and A. Isogai (2004). "TEMPO-mediated oxidation of native cellulose. The effect of oxidation conditions on chemical and crystal structures of the water-insoluble fractions." Biomacromolecules 5(5): 1983-1989.

Saito, T., S. Kimura, Y. Nishiyama and A. Isogai (2007). "Cellulose nanofibers prepared by TEMPO-mediated oxidation of native cellulose." Biomacromolecules 8(8): 2485-2491.

Sehaqui, H., M. Allais, Q. Zhou and L. A. Berglund (2011). "Wood cellulose biocomposites with fibrous structures at micro-and nanoscale." Composites Science and Technology 71(3): 382-387.

Shinoda, R., T. Saito, Y. Okita and A. Isogai (2012). "Relationship between length and degree of polymerization of TEMPO-oxidized cellulose nanofibrils." Biomacromolecules 13(3): 842-849.

Spence, K. L., R. A. Venditti, O. J. Rojas, Y. Habibi and J. J. Pawlak (2011). "A comparative study of energy consumption and physical properties of microfibrillated cellulose produced by different processing methods." Cellulose 18(4): 1097-1111.

Svagan, A. J., M. A. Samir and L. A. Berglund (2008). "Biomimetic foams of high mechanical performance based on nanostructured cell walls reinforced by native cellulose nanofibrils." Advanced Materials 20(7): 1263-1269.

Torvinen, K., J. Sievänen, T. Hjelt and E. Hellén (2012). "Smooth and flexible filler-nanocellulose composite structure for printed electronics applications." Cellulose 19(3): 821-829.

Azetsu, A.; Koga, H.; Isogai, A.; Kitaoka, T. Synthesis and Catalytic Features of Hybrid Metal Nanoparticles Supported on Cellulose Nanofibers. Catalysts 2011, 1 (1): 83-96.

Yeh, Y.-C., Creran, B., & Rotello, V. M. (2012). Gold Nanoparticles: Preparation, Properties, and Applications in Bionanotechnology. Nanoscale,4(6): 1871–1880.

Daniel MC, Astruc D. (2014). Gold nanoparticles: assembly, supramolecular chemistry, quantum-size-related properties, and applications toward biology, catalysis, and nanotechnology. Chem Rev. , 104(1):293-346.

Ngo YH, Li D, Simon GP, Garnier G. (2011). Paper surfaces functionalized by nanoparticles. Adv Colloid Interface Sci., 163(1):23-38

Serrano Rubio, Aída. Modified Au-based nanomaterials studied by surface plasmon resonance spectroscopy: Estudio de nanomateriales modificados basados en Au mediante espectroscopia de resonancia de plasmones de superficie. Madrid: Universidad complutense de Madrid. Departament de física de materials. 2014 <<http://hdl.handle.net/10261/104320>> [Consulta: 30 de maig de 2015]

Sfanji, Asmae. Producció caracterització i aplicació superficial de les nanofibres de cel·lulosa: determinació de propietats del nou suport. Girona: Universitat de Girona. Departament d'enginyeria química, agrària i tecnologia agroalimentària. 2014.

Al-Qadi, Sonia y Remuñán-López Carmen. 7. Nanopartículas metálicas: oro. Dins Monografías de la real academia nacional de farmacia. (p. 223-248). Universidad de Santiago de Compostela. Departamento de Farmacia y Tecnología Farmacéutica, 2014.

González Tovar, Israel. Production and characterization of nanofibrillated cellulose from eucalyptus fibres and its application on papermaking. Girona: Universitat de Girona. Departament d'enginyeria química, agrària i tecnologia agroalimentària, 2014.

BioNavis Oy Ltd.(2015) *How does Surface Plasmon resonance work?*. Recuperat des de <http://www.bionavis.com/technology/spr/>